

Master's Thesis

Catalytic Investigations Regarding Alternative Bed Materials for Dual Fluidized Bed Gasification of Biomass

ausgeführt zum Zwecke der Erlangung des akademischen Grades eines Diplom-Ingenieurs

unter der Leitung von

Univ.Prof. Dipl.-Ing. Dr.techn. Hermann Hofbauer

unter der Betreuung von

Dipl.-Ing. Matthias Kuba

Institut für Verfahrenstechnik, Umwelttechnik und technische Biowissenschaften

E 166

eingereicht an der Technischen Universität Wien

Fakultät für Maschinenwesen und Betriebswissenschaften

von

Fabian Havlik

Matrikelnummer: 9471371

Schüttelstraße 27/21

1020 Wien

Wien, am 2015

Fabian Havlik

Kurzfassung

Diese Diplomarbeit befasst sich mit der Untersuchung zur Eignung von alternativen Bettmaterialien für die Zweibettwirbelschicht-Dampfvergasung. Frisches und gebrauchtes Olivin, frischer und gebrauchter Quarzsand sowie Kalziumoxid werden auf ihre katalytische Aktivität untersucht. Gebrauchte Materialien kamen bereits in einer Wirbelschicht zum Einsatz und weisen eine kalziumreiche Schicht um das Partikel auf.

Die Bettmaterialien werden in einem kontinuierlich betriebenen Reaktor bei Temperaturen zwischen 750°C und 850°C mit Wasserdampf und Kohlenwasserstoffen durchströmt. Dabei werden drei Reaktionen nachgebildet:

- Wassergas Shift Reaktion
- Steam Reforming von Ethen
- Steam Reforming von Toluol

Diese drei Reaktionen wurden gewählt um die Vielzahl der im Reaktor ablaufenden Reaktionen zu repräsentieren. Die Wassergas Shift Reaktion stellt die einfachst nachzubildende Reaktion dar. Steam Reforming von Ethen soll das Steam Reforming von leichteren Kohlenwasserstoffen und Steam Reforming von Toluol das Steam Reforming von schwereren Kohlenwasserstoffen (Teere) repräsentieren.

Der Umsatz wird mit einem 5-Komponenten-Gasmessgerät ausgewertet und verglichen. Gemessen wird der nach der Reaktion entstandene Volumsanteil von Wasserstoff, Kohlendioxid, Kohlenmonoxid, Methan und Sauerstoff.

Die Auswertung der Ergebnisse zeigt einen Zusammenhang zwischen den drei durchgeführten Reaktionen und stellt den Unterschied zwischen beschichteten und unbeschichteten Bettmaterialien dar.

Abstract

This master's thesis deals with the investigation of alternative bed materials for dual fluidized bed gasification. Fresh and used olivine, fresh and used quartz sand as well as calcium oxide are investigated regarding their catalytic activity. The used bed materials have already been in operation in a fluidized bed and are coated with a calcium-rich layer.

The different bed materials are located in a continuously driven glass reactor and are surrounded by steam and hydrocarbons. The glass reactor will be held at temperatures between 750°C and 850°C. The following reactions are recreated:

- water-gas shift reaction
- steam reforming of ethene
- steam reforming of toluene

These reactions were chosen to represent the multitudes of reactions in the reactor. The water-gas shift reaction is the easiest reaction to reproduce. Steam reforming of ethene is supposed to represent steam reforming of lighter hydrocarbons and steam reforming of toluene is supposed to represent steam reforming of heavier hydrocarbons (tars).

The conversion rate is measured with a five-component-gas-analyzer. The volume fraction of hydrogen, carbon dioxide, carbon monoxide, methane and oxygen is measured after the reaction. The evaluated results show a connection between those three reactions and present a difference between coated and non-coated bed materials.

Contents

List of Figures	viii
List of Tables	ix
List of Abbreviations	x
1 Introduction	1
1.1 Motivation	1
1.2 Aim of the Work	2
2 Fundamentals	4
2.1 Gasification and other Thermochemical Processes	4
2.1.1 Comparing Combustion, Gasification and Pyrolysis	4
2.1.2 Gasifying Mediums	5
2.1.3 Reactions	6
2.2 Gasification Reactors	8
2.2.1 Fixed Bed Gasification	8
2.2.2 Fluidized Bed Gasificaton	11
2.2.3 Dual Fluidized Bed Gasification	13
2.2.4 Entrained Flow Gasification	16
2.3 Bed Material	16
2.4 Previous Studies	18
3 Materials and Methods	20
3.1 Reactions	20
3.2 Bed Materials	21
3.3 Equipment	22
3.3.1 Description and Operation	22
3.3.2 Adaptions	23

3.4	Procedure	27
3.4.1	Flow Rate Calculation	27
3.4.2	Water-Gas Shift Reaction	27
3.4.3	Steam Reforming of Ethene	28
3.4.4	Steam Reforming of Toluene	28
3.4.5	Flow Sheet	30
3.5	Simulation	31
4	Results	33
4.1	Water-Gas Shift Reaction	33
4.1.1	Simulation Results	33
4.1.2	Experimental Results	34
4.2	Steam Reforming of Ethene	39
4.2.1	Simulation Results	39
4.2.2	Experimental Results	39
4.3	Steam Reforming of Toluene	43
4.3.1	Simulation Results	43
4.3.2	Experimental Results	44
4.4	Comparison	50
5	Discussion	53
5.1	Water-Gas Shift Reaction	53
5.2	Steam Reforming of Ethene	54
5.3	Steam Reforming of Toluene	55
5.4	Comparison of Reactions and Bed Material	56
5.5	Error Analysis	57
5.5.1	Systematic Errors	57
5.5.2	Operating and Evaluation Errors	57
5.5.3	Simplifications	58
5.5.4	Relevant Errors	58

6 Conclusion and Outlook	59
References	62
Appendix A, Results of Water-Gas Shift Reaction Tests	63
Appendix B, Results of Steam Reforming of Ethene Tests	69
Appendix C, Results of Steam Reforming of Toluene Tests (water/toluene ratio: 7/1)	75
Appendix D, Results of Steam Reforming of Toluene Tests (water/toluene ratio: 14/1)	78

List of Figures

1	Gasification process with continuative processing, adapted from [13]	1
2	Temperature areas of thermochemical processes, adapted from [13]	5
3	Gasifying mediums and process conditions, adapted from [13]	6
4	Reaction equilibrium of the water-gas shift reaction depending on the temperature, adapted from [13]	7
5	Sub-processes in an updraft gasifier and temperature gradient [1]	9
6	Sub-processes in an downdraft gasifier and temperature gradient [1]	10
7	Comparison of a bubbling fluidized bed (left) and a circulating fluidized bed (right), adapted from [13]	12
8	Operation principle of the DFB gasification process (Vienna University of Technology)	14
9	Scheme of reactors (Vienna University of Technology)	15
10	Combustion zone and gasification zone [1]	16
11	Entrained flow gasifier [1]	17
12	Test rig for experiments	24
13	Syringe pump for toluene injection	25
14	Tee-connector to mix nitrogen with toluene	26
15	Constructing a toluene evaporator	26
16	Actual flow sheet of the test rig and its compounds (Vienna University of Technology)	30
17	Flow sheet of the water-gas shift reaction in the COCO simulation environment	31
18	Flow sheet of steam reforming of ethene in the COCO simulation environment	32
19	Flow sheet of steam reforming of toluene in the COCO simulation environment	32
20	COCO-Simulation result of the water-gas shift reaction	33
21	Volumetric composition at 750°C reactor temperature	36
22	Volumetric composition at 800°C reactor temperature	36

23	Volumetric composition at 850°C reactor temperature	37
24	Molar proportion of hydrogen in the product gas	37
25	Molar proportion of carbon dioxide in the product gas	38
26	Carbon monoxide conversion rate	38
27	COCO-Simulation results of steam reforming of ethene combined with the water-gas shift reaction	39
28	Volumetric composition at 750°C reactor temperature	41
29	Volumetric composition at 800°C reactor temperature	41
30	Volumetric composition at 850°C reactor temperature	42
31	Volumetric proportion of hydrogen in the product gas	42
32	COCO-Simulation results of steam reforming of toluene combined with the water-gas shift reaction at a molar water/toluene ratio of 7/1	43
33	-COCO-Simulation results of steam reforming of toluene combined with the water-gas shift reaction at a molar water/toluene ratio of 14/1	44
34	Volumetric composition at 750°C reactor temperature and 7/1 water/toluene ratio	46
35	Volumetric composition at 750°C reactor temperature and 14/1 water/toluene ratio	46
36	Volumetric composition at 800°C reactor temperature and 7/1 water/toluene ratio	47
37	Volumetric composition at 800°C reactor temperature and 14/1 water/toluene ratio	47
38	Volumetric composition at 850°C reactor temperature and 7/1 water/toluene ratio	48
39	Volumetric composition at 850°C reactor temperature and 14/1 water/toluene ratio	48
40	Volumetric proportion of hydrogen in the product gas at a water/toluene ratio of 7/1	49

41	Volumetric proportion of hydrogen in the product gas at a water/toluene ratio of 14/1	49
42	Volumetric proportion of hydrogen with used quartz sand as catalyst . . .	51
43	Volumetric proportion of hydrogen with fresh olivine as catalyst	51
44	Volumetric proportion of hydrogen with used olivine as catalyst	52
45	Volumetric proportion of hydrogen with calcium oxide as catalyst	52

List of Tables

1	Calculated flow rates for the water-gas shift reaction	27
2	Calculated flow rates for steam reforming of ethene	28
3	Calculated flow rates for steam reforming of toluene	28
4	Calculated flow rates for steam reforming of toluene combined with the water-gas shift reaction	29

List of Abbreviations

Symbol	Meaning
\dot{m}	mass flow
M	molar mass
X	conversion rate
\dot{n}	molar flow
\dot{V}	volume flow
ΔH	standard enthalpy of reaction
λ	air/fuel ratio
ρ	density
DFB	Dual Fluidized Bed
COCO	Cape Open to Cape Open simulation environment
CaO	calcium oxide
C	carbon
CO	carbon monoxide
CO_2	carbon dioxide
CH_4	methane
C_2H_4	ethene
C_7H_8	toluene
H_2	hydrogen
H_2O	water
N_2	nitrogen
O_2	oxygen

1 Introduction

1.1 Motivation

To cover the rising demand of energy, the use of renewable energies will become more important. Resigning on fossil fuels in a sustainable way affords a mix of regenerative energies. Energy from solid biomass is one possibility to raise the ratio of regenerative energy. Beside the classic energy generation out of incineration, biomass can also be converted in a secondary energy carrier by gasification. This can bring up some advantages in terms of handling and further conversion to heat, electricity or fuels. The outcome of this is a wider and more flexible use of biomass as a primary energy carrier. Figure 1 shows a possible gasification process with continuative processing.

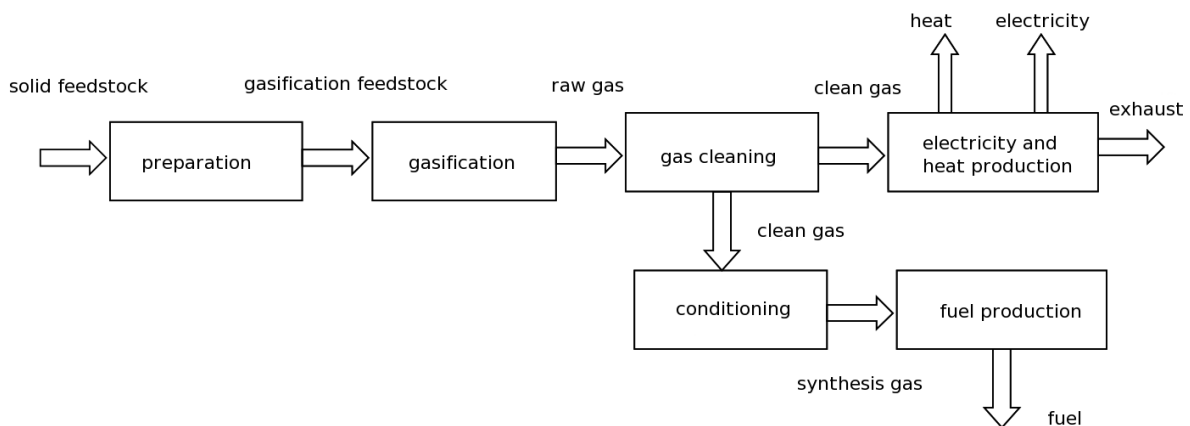


Figure 1: Gasification process with continuative processing, adapted from [13]

The dual fluidized bed (DFB) gasifier is a promising technology for regenerative energy production by gasification. The fluidized bed is divided into a gasification and a combustion zone. Between those two zones a bed material, which acts as heat carrier and catalyst, is circulating. With the DFB gasifier biomass can be used either as energetic source or as a material source to produce fuels, methane or hydrogen. This technology, which was developed at the University of Technology in Vienna, is demonstrated in industrial scale since 2001. [7]

Today mineral olivine, which is a magnesium iron silicate, is applied as circulating bed material. Olivine was chosen because of its good catalytic properties, its possibility to act as a heat carrier and its abrasive strength. Its disadvantages are higher costs compared to quartz sand and the matter of fact, that ash which came into contact with olivine has to be treated as hazardous waste.

Previous studies showed a modification of the bed material due to its interaction with biomass ash and additives. This interaction results in the formation of calcium-rich layers on the bed material. In the past it was shown that this coating on olivine particles enhances the catalytic activities during the water-gas shift reaction. [5,16]

This statement is the base for the assumption, that catalytic activity is depending on the coating of the bed material. Thus, every material, which resists the upcoming heat and abrasion and on which a calcium-rich layer can form on, would be applicable.

1.2 Aim of the Work

The aim of this work is to show that other bed materials beside olivine have the potential to be used in a DFB gasifier according to catalytic tests. Different fresh and also used (coated) bed materials, such as olivine, quartz sand and calcium oxide are tested to prove their ability to enhance the water-gas shift reaction respectively the steam reforming of ethene or toluene. An interesting alternative is quartz sand, which causes lower cost in terms of acquisition and ash treatment. Quartz sand has no catalytic properties, but is a good heat carrier and resistant to abrasion.

Therefore three reactions will be studied: water-gas shift reaction, steam reforming of ethene and steam reforming of toluene. Additionally, a correlation between those reaction is figured out. Thus, a prediction for other reactions could be made if the conversion of one reaction with a certain catalyst is known.

Subsequently, two questions are to be answered with this work:

- Is coating of the bed material a relevant factor to improve overall catalytic properties? Have different bed materials the same catalytic properties as long as they are coated?

- Is there a correlation between the water-gas shift reaction, steam reforming of ethene and steam reforming of toluene?

These results are a basic approach for further improvements on the DFB gasifier.

2 Fundamentals

2.1 Gasification and other Thermochemical Processes

Gasification is the conversion of liquid or solid feedstock (e.g. carbon C) into useful chemical feedstock or gaseous fuel. This product is called product gas or synthesis gas which contains low-molecular-weight gases like carbon monoxide and hydrogen. For gasification a gasifying medium like air, steam or oxygen is needed. If no gasifying medium is used the process is called pyrolysis which is a thermal decomposition process.

Gasification and combustion are both thermochemical processes. The main difference is that gasification packs energy into the product gas as chemical bonds and combustion breaks chemical bonds to release energy. The product gas of the gasification process can be used at another time on another place to release energy. Combustion creates flue gas which can not be used for further processing. [1, p.199]

2.1.1 Comparing Combustion, Gasification and Pyrolysis

Combustion, gasification and pyrolysis can be characterised by the air/fuel ratio λ . Combustion takes place when the amount of air exceeds the amount of fuel ($\lambda \geq 1$). The gasification process needs less air than needed for a full combustion ($0 < \lambda < 1$), if the gasifying medium is air. If the gasifying medium is not air, the air/fuel ratio is obsolete. Pyrolysis doesn't need air and the air/fuel ratio is zero ($\lambda = 0$). [13, p.375]

Combustion is an exothermic reaction - it releases heat. On the other hand heat has to be supplied for gasification and pyrolysis, which are both endothermic reactions. [1, p.199]

Figure 2 shows the temperature area where pyrolysis, gasification and combustion take place. The operation temperature for pyrolysis (200°C–600°C) is lower than for gasification (500°C–1000°C). Combustion occurs at high temperatures around 700°C to 1200°C. [13, p.380]

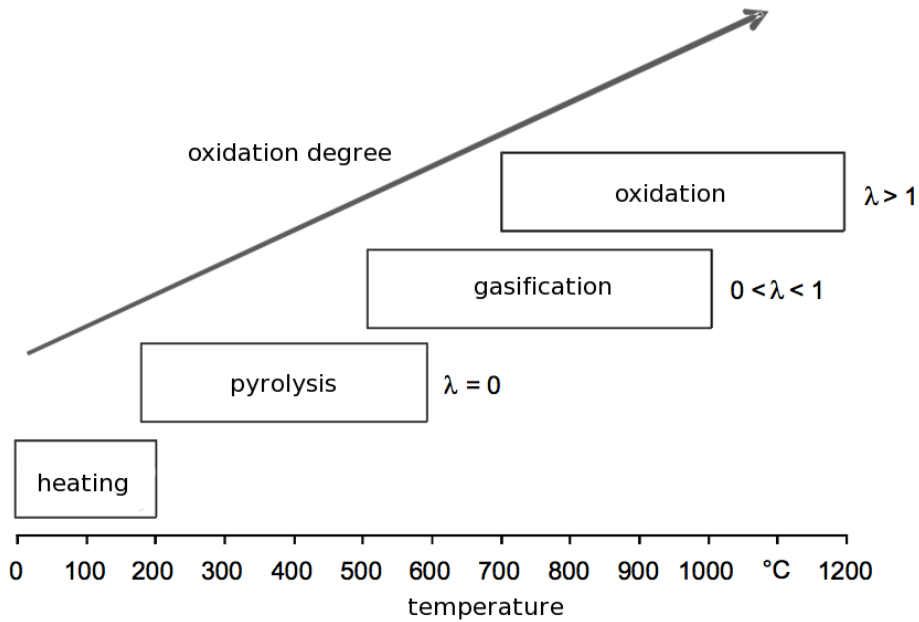


Figure 2: Temperature areas of thermochemical processes, adapted from [13]

2.1.2 Gasifying Mediums

Gasifying mediums react with carbon and heavy hydrocarbons to low-molecular-weight hydrocarbons and hydrogen (product gas). The main gasifying mediums are:

- Oxygen O_2
- Steam H_2O
- Air
- Carbon dioxide CO_2

If oxygen is used, the product gas includes carbon monoxide CO for low oxygen and carbon dioxide CO_2 for high oxygen. The same relation with an additional high amount of nitrogen N_2 in the product gas is valid for air as a gasifying medium. The gasification process will become a combustion process by exceeding the stoichiometric amount of oxygen. [1, p.200]

If steam is used, the product gas contains more hydrogen H_2 per unit of carbon. Carbon monoxide CO and hydrogen H_2 will be the predominant gases in the product gas. [1, p.200]

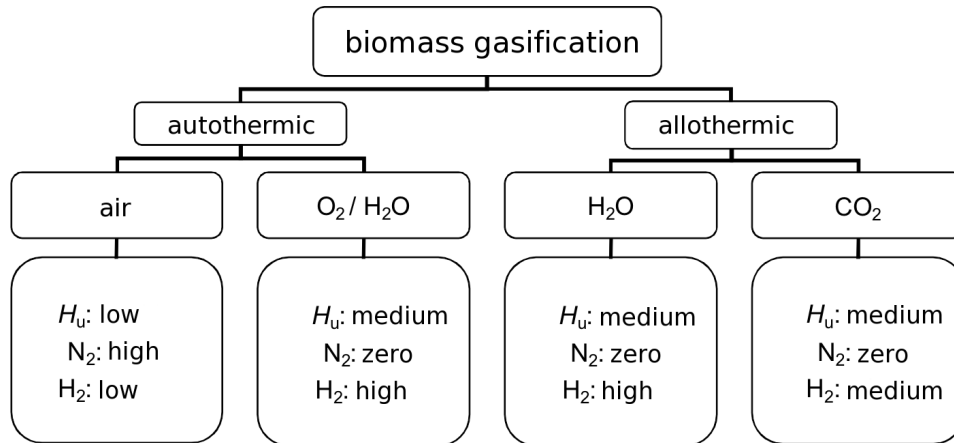
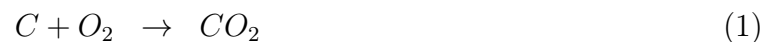


Figure 3: Gasifying mediums and process conditions, adapted from [13]

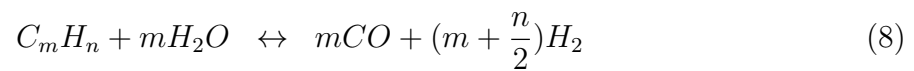
Figure 3 shows the correlation between gasifying medium and process conditions. If the gasifying medium is air or oxygen O_2 , no extra heat has to be added (autothermic process). If the gasifying medium is steam H_2O or carbon dioxide CO_2 , heat has to be supplied to run the process (allothermic process).

2.1.3 Reactions

During gasification, several reactions occur. Depending on temperature and pressure different reactions emerge partially or full. The following reactions (equations 1-5) have carbon as reactant, representing solid feedstock. [13, p.390]



Products of this gas-solid-reactions are gases, which will be converted in further gas-gas-reactions listed below.



Depending on the gasifying medium not all of those reactions occur. For this work the gas-gas-reactions are essential. The water-gas shift reaction (equation 6) ($\Delta H = -41,5kJ/mol$) [8] and the methanation reaction (equation 7) ($\Delta H = -203,0kJ/mol$) [13] are exothermic. The standard enthalpy of steam reforming of hydrocarbons (equation 8) depends on its reactant. Steam reforming of toluene is an endothermic reaction ($\Delta H = 869,8kJ/mol$) [18].

The reaction equilibrium depends on pressure and temperature. As an example, figure 4 shows the equilibrium of the water-gas shift reaction. As the reaction is exothermic, the equilibrium is on the side of the reactant at high temperatures.

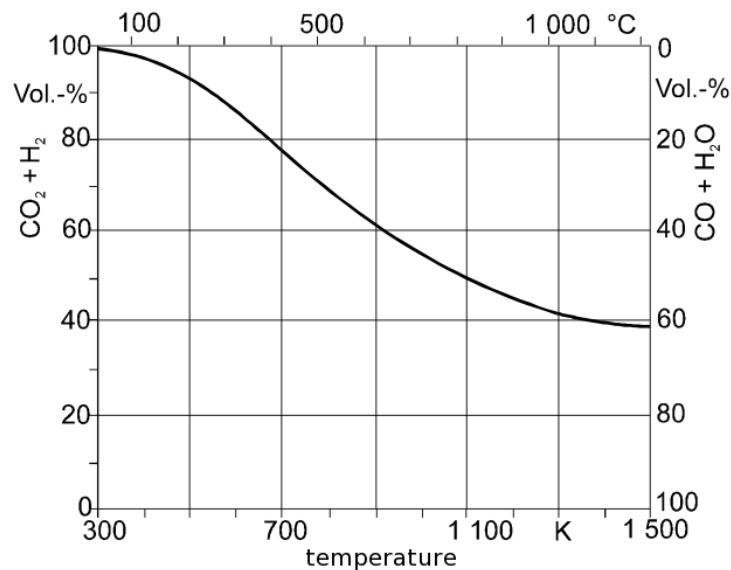


Figure 4: Reaction equilibrium of the water-gas shift reaction depending on the temperature, adapted from [13]

The reactions used for the experiments are described in chapter 3.

2.2 Gasification Reactors

Gasification reactors can be classified by means of

- the type of the reactor, which is defined by the way of contact between gasifying medium and biomass.
- the heat supply. This can be an internal (autothermic) or an external (allothermic) heat source.
- the deployed gasifying medium.
- the pressure in the gasification reactor (atmospheric pressure or overpressure).

In literature, a classification according to the type of the reactor is the most common. Consecutively this classification is chosen for this work. [13, p.602]

2.2.1 Fixed Bed Gasification

Solid fuel particles are fed into the reactor and are not moved by the gasifying medium stream. This can be realized through big fuel particles or small gas flow rates. The solid biomass is usually inserted at the top and moves because of gravitation and continuous decomposition slowly to the bottom. As a result, different sub-processes occur areal separated. The gasifying medium stream is either performed as counter current flow for an updraft gasifier or direct current flow for an downdraft gasifier. [13, p.603]

Updraft Gasifier In an updraft gasifier, fuel is fed from the top and the gasifying medium streams slightly preheated through a grid in the bottom to result as counter current flow. Therefore, clearly seperated reaction zones emerge in the reactor where primarily sub-processes run, showed in figure 5. Product gas leaves at the top. [13, p.603]

Oxidation is taking place in the combustion zone and the required heat for the total gasification process is generated. The heated gas, which is a mix of the gasifying medium and the flue gas of the combustion zone, transports heat to the gasification zone and other zones. Additionally, formed carbon dioxide CO_2 is partially converted to carbon

monoxide CO and steam H_2O is partially converted to hydrogen H_2 and carbon monoxide CO . On its way to the top, the gas is passing progressively colder zones and finally leaves as product gas with relatively low temperatures about $100^\circ C$ to $200^\circ C$. Therefore the overall efficiency is relatively high. [13, p.603]

A high geometric range of solid fuel parts (2cm to 20cm) can be used. The water content can be up to 60% because the water is entrained by the gas stream and doesn't pass the hot reduction zone. [13, p.603]

A disadvantage of this process is the high amount of condensible parts (e.g. tars) in the product gas. Volatile matter, which form in the pyrolysis zone, come directly into the product gas, without passing the reduction zone. To remove those condensible parts, complex gas cleaning processes are needed. [13, p.603]

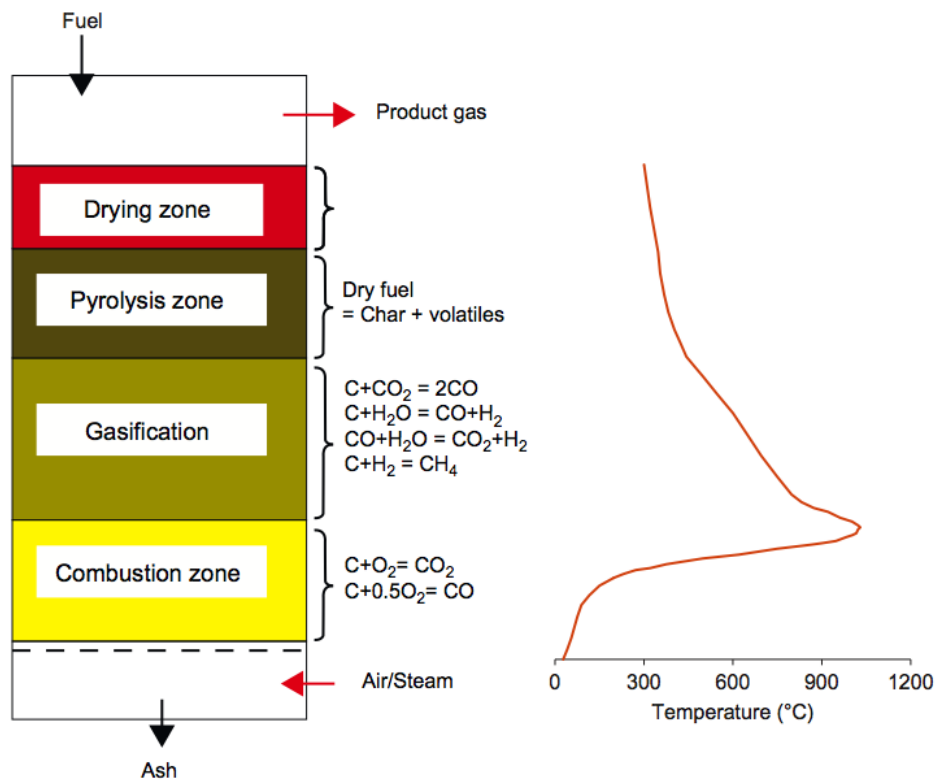


Figure 5: Sub-processes in an updraft gasifier and temperature gradient [1]

Downdraft Gasifier The difference to an updraft gasifier is, that the gasifying medium flows into the same direction like the fuel moves. The gasifying medium is inserted lateral and the product gas leaves at the bottom. Reaction zones emerge in a different order compared to the updraft gasifier, see figure 5. [13, p.606]

The oxidation, which provides heat, is taking place where the gasifying medium is inserted. Above the combustion zone, the temperature highly decreases, because the gas streams downwards and doesn't provide heat in upper zones. Long organic bonds, which formed in the pyrolysis zone come directly into the combustion zone. Most of them will be separated into shorter hydrocarbons and tars get reduced. [13, p.606]

Product gas leaves at relatively high temperatures (600°C to 800°C). This heat can only be used to heat up the gasification medium. Thus, the overall efficiency is lower than in an updraft gasifier. [13, p.606]

Solid fuel has to be geometrically defined (3cm x 3cm x 5cm) and the water content has to be lower than 20% because a steady temperature gradient is needed within the particular process zones to achieve a good gas quality. [13, p.606]

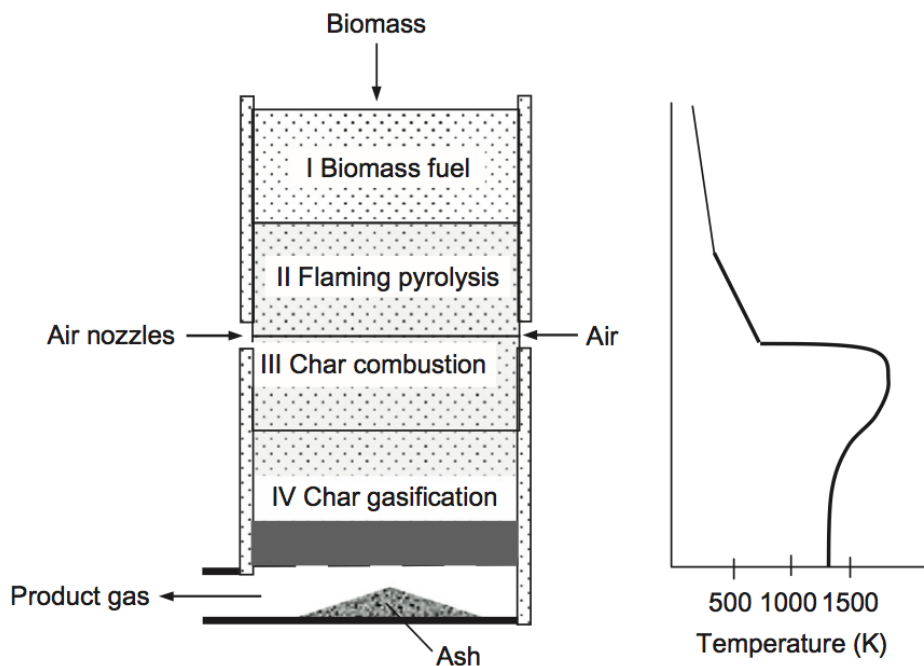


Figure 6: Sub-processes in an downdraft gasifier and temperature gradient [1]

2.2.2 Fluidized Bed Gasification

The bed consists of dispersed bed material (e.g. quartz sand). If the gasifying medium streams with sufficient speed through the gasifier, the fluidized bed develops. Solid fuel is inserted in small parts or particles and mixes instantly with the bed material. Compared to fixed bed gasifiers, no distinct temperature or reaction zones arise. All partial reactions run parallel in the whole reactor with temperatures between 700°C and 900°C. The constant temperatures and the easy temperature control are the main advantages of a fluidized bed gasifier. [13, p.609]

Because of the high specific surface of the particles and the good conduction of heat from bed material to fuel particles, the retention time can be very short (some seconds up to minutes). The gasification can either be under atmospheric pressure or overpressure. The operation with overpressure (e.g. 30bar) allows smaller reactor design for the same output. In addition, the product gas is already under pressure. Nevertheless, high technical effort is needed and therefore it is only for large facilities reasonable. [13, p.609]

The product gas leaves at high temperatures. To use the heat energy, heat exchanger can be installed. The tar ratio is higher than in comparable downdraft gasifiers, but definite lower than in updraft gasifiers. [13, p.609]

Fluidized bed gasifier can be subclassified into two types:

- Bubbling fluidized bed gasifier
- Circulating fluidized bed gasifier

Figure 7 shows a schematic drawing of those two systems.

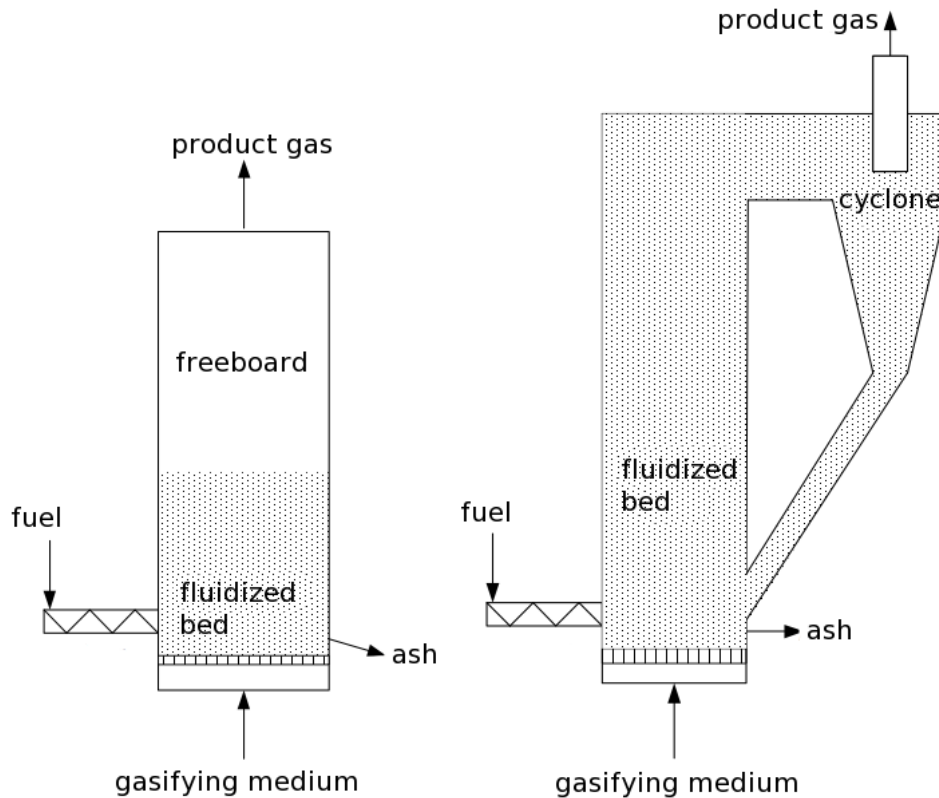


Figure 7: Comparison of a bubbling fluidized bed (left) and a circulating fluidized bed (right), adapted from [13]

Bubbling Fluidized Bed Gasifier The stream velocity of the gasifying medium has to be in-between the loosening velocity (minimal velocity to hold the fluidized bed) and the floating velocity of a single bed material particle. Practically, a stream velocity 5 to 15 times the loosening velocity is proven. Because of the geometrically well defined bed material, solid fuel particles can be in a range between 1mm to 70mm. [13, p.611]

Solid fuel is inserted by a spiral conveyor or thrown into the freeboard. Fuel particles get dried instantly and pyrolytic decomposition takes place. Gases which leave the fluidized bed might continue reacting in the freeboard because of high temperatures. If the residence time is high, the tar ratio will be low. A notable amount of particles and ash leave the reactor. Hence, particle separation is required. [13, p.611]

Circulating Fluidized Bed Gasifier In a circulating fluidized bed, the stream velocity is higher than the floating velocity of a single bed material particle. Thus, no bed surface is present. The fluidized bed is unequally spread over the whole reactor. At the bottom of the reactor, a denser zone of the fluidized bed forms than at the top. Because of high gas velocities, the bed material is dragged-out of the reactor. Afterwards, it gets separated from the gas stream by a cyclone and recycled into the reactor. [13, p.613]

Solid fuel is inserted by a spiral conveyor. The thermo-chemical process runs at defined temperatures in the whole fluidized bed. The product gas leaves through a cyclone at the top. [13, p.613]

2.2.3 Dual Fluidized Bed Gasification

The major problem of gasification with air as a gasifying medium is that the product gas is diluted with nitrogen. A gasification with oxygen would solve that problem, but holds high costs. Another solution is to separate combustion and gasification in different reactors. The dual fluidized bed gasification is a combination of two fluidized bed gasifiers. One fluidized bed is operated as a steam gasifier and in the other fluidized bed fuel is burned to provide heat. The heat transport is either realized by a circulating bed material between those two reactors or by a high temperature transfer with heat pipes. [13, p.614]

At the Munich University of Technology, temperature transport with heat pipes was investigated. The Biomass Heatpipe Reformer (BioHPR) was developed. The aim of this project was to integrate the technology of liquid metal heat pipes in the gasification process. Further exergetic analysis of where carried out. [10, 14]

Another method is the heat transport by bed material. The bed material circulates between the two reactors and transports heat from the combustion reactor to the gasification reactor. Based on this principle the Dual Fluidized Bed (DFB) gasification process was developed at the Vienna University of Technology. Its aim is to produce a high grade synthesis gas from solid fuels. Figure 8 shows the operation principle of the DFB gasification. [7]

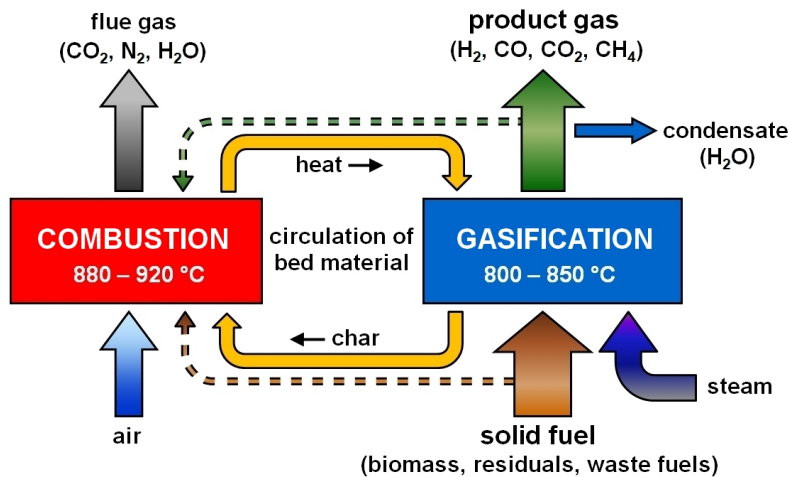


Figure 8: Operation principle of the DFB gasification process (Vienna University of Technology)

An industrial demonstration plant was built in 2001 in Güssing, Austria, by the Institute of Chemical Engineering, Vienna University of Technology. It is a 8MW fuel power plant which can provide 2MW_{el} power and $4,5\text{MW}_{\text{th}}$ heat for the district heating system. The plant runs in commercial operation. Figure 9 shows the scheme of the reactors in Güssing.

Fuel is inserted into the gasification reactor and combustion reactor. The bed material slides from the gasification reactor into the combustion reactor. High air stream velocities transport it to the top followed by a cyclone. Inserted fuel gets entrained and burned. The cyclone separates the flue gas and the bed material, which falls back into the gasification reactor. Because of the provided heat from the bed material, the solid fuel is gasified with steam as gasifying medium. [7]

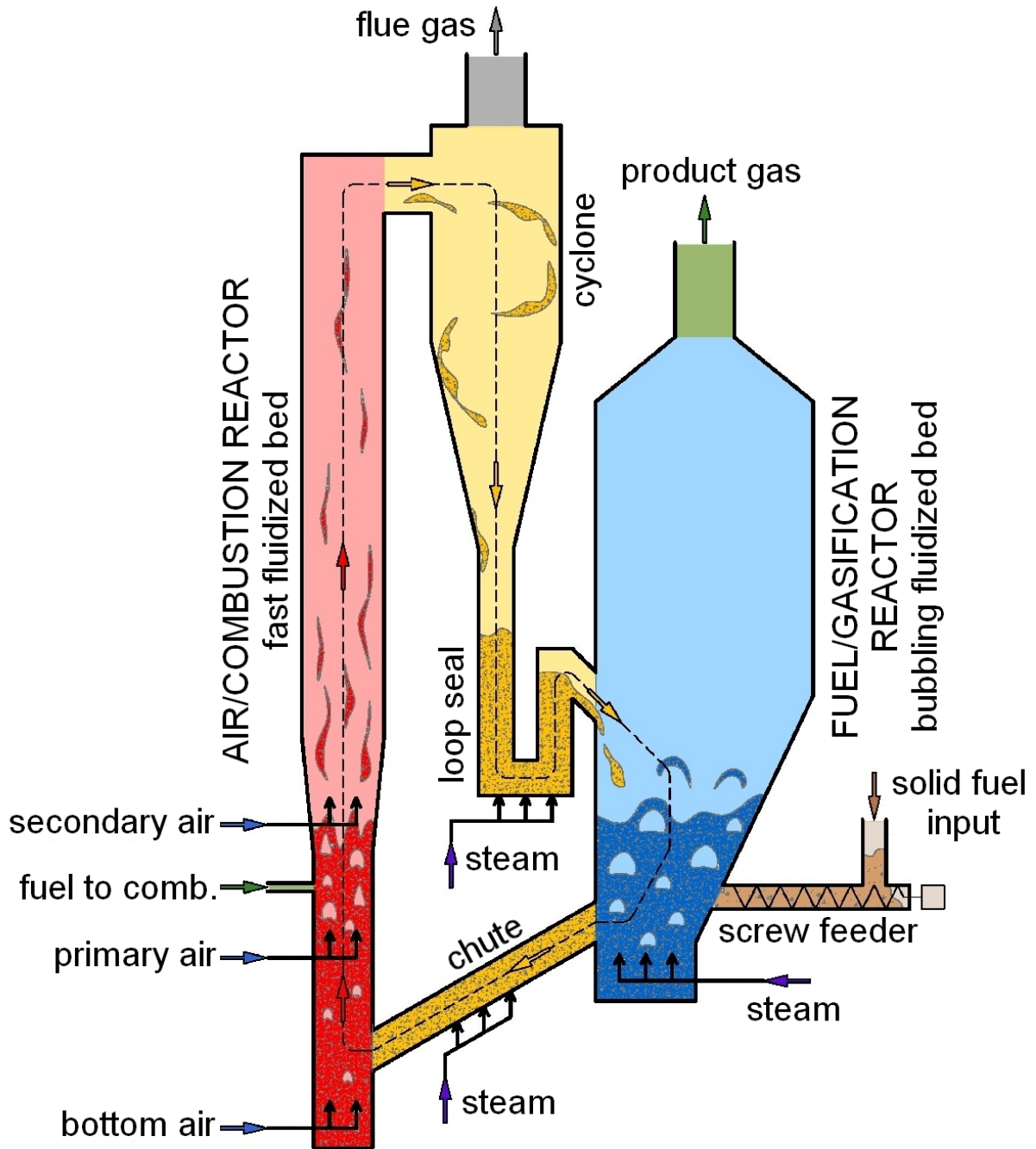


Figure 9: Scheme of reactors (Vienna University of Technology)

2.2.4 Entrained Flow Gasification

Grinded solid fuel particles get inserted in the reactor and entrained by the gasifying medium. The operating temperatures are 1200°C to 2000°C and the gasification instantly takes place in the reactor. The gas velocity is sufficiently high to fully carry away the fuel particles. In the reactor, the combustion zone with the highest temperatures is directly after the burner. Connected to the combustion zone, the gasification zone develops (Figure 10). A schematic of an entrained flow gasifier is shown in figure 11. [13, p.617]

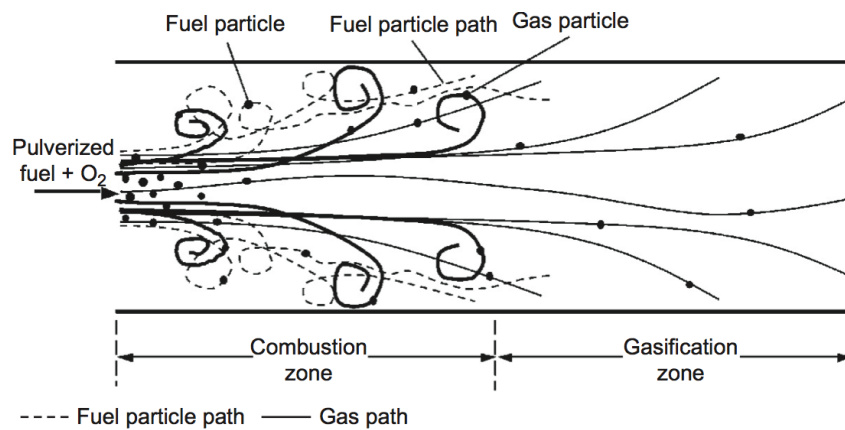


Figure 10: Combustion zone and gasification zone [1]

Entrained flow gasifiers are mostly used in integrated gasification combined cycle (IGCC) plants. They are useful for large-scale gasification of coal, petroleum coke and refinery residues. They can be operated at higher pressures of 20bar to 70bar. Because of the higher temperature and pressure, higher technical effort is needed. [1, p.268]

2.3 Bed Material

Bed materials are needed to evenly distribute heat and fuel particles in the reactor. Bed materials can either be inert (e.g. quartz sand) or catalytic active. In the FICFB reactor a catalytic active bed material is used. The catalytic effect leads to a higher conversion rate in the gasification zone. Currently, olivine, a magnesium iron silicate, is proven. Additionally to its catalytic functions, it is a good heat carrier and has a good abrasion resistance. [17, 19]

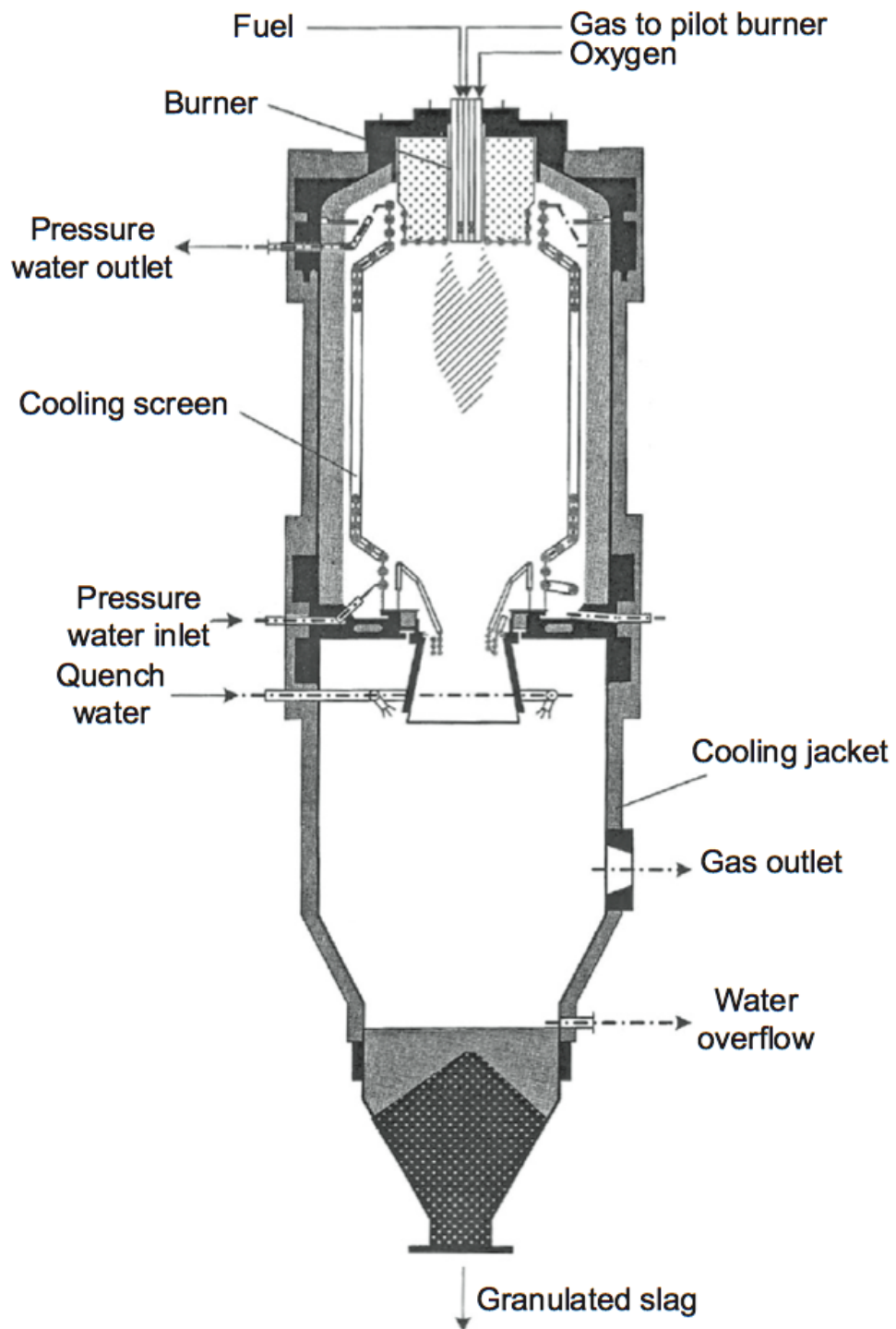


Figure 11: Entrained flow gasifier [1]

2.4 Previous Studies

Bed Material Research at the Institute of Chemical Engineering, Vienna University of Technology showed that bed material which is in use in a DFB gasifying plant have calcium-rich layers after a certain amount of operating hours. This coating is induced by biomass ash. Bed material coating leads to different catalytic effects and is also a precursor for bed agglomeration. [3]

Further tests examined the difference of coated and fresh olivine. In a pilot plant, lower tar content in the product gas was measured by using coated olivine as bed material. [4]

Calcium-rich layers on olivine particles lead to a higher catalytic effect. An intensive contact of olivine particles and ash promotes the formation of the layers in the combustion reactor. [3]

At the Lulea University of Technology (Sweden) and the Umea University of Technology (Sweden), bed particle layer formation depending on operating time was investigated. It was shown, that after one day of operation, only a thin layer formed around bed particles, which increased with operation time. During the first operation days, the layer growth rate was high, but decreased over time. [6]

A closer look on the water-gas shift reaction by using fresh olivine, used olivine and calcite as catalyst were investigated at the Vienna University of Technology. Carbon monoxide CO conversions up to 61,5% were achieved for calcite. Used olivine showed similar behaviour. Fresh olivine showed carbon monoxide CO conversion rates less than 20%. [16]

Bed agglomeration was investigated at the Department of Chemical Engineering, Combustion Chemistry Research Group at Abo Akademi University (Finland). Ash behaviour modelling with seven biomass fuels under reducing, pressurised conditions in fluidized bed gasification were examined by means of thermodynamic multi-phase multi-component equilibrium (TPCE) calculations. The calculations can be used as guidelines for predicting bed agglomeration. Further, the model was compared with pilot-scale experiment in a pressurised fluidized bed gasifier and in an atmospheric test rig. This verified the use of the calculation model. [11,12]

Tar Formation Condensable hydrocarbons (tars) lead to an restriction in plant operation. Condensed tars cause accumulation and contamination in plant parts (e.g. heat exchangers). The impact of olivine regarding the product gas and distribution of condensable hydrocarbons (tars) was studied at the Vienna University of Technology. Quartz sand, which is considered to be inert, was taken as a reference. The experimental device was a pilot plant of 100kW fuel input. The study showed the positive tar reducing effects of olivine compared with quartz sand as a reference point. [17, 19]

Researches at the North China Electric Power University (China) used a nickel supported catalyst ($\text{Ni-CeO}_2/\text{SBA-15}$) for steam reforming of toluene, which represents a model compound of tar. The tests were run in a lab-scale test rig. The maximum toluene conversion of 98,9% was found at the highest tested temperature of 850°C. The product gas contained mainly hydrogen H_2 and carbon monoxide CO together with a little of carbon dioxide CO_2 and methane CH_4 . [9]

Similar experiments were conducted at the Energy Research Institute of Shandong Academy of Sciences (China). Thereby, a maximum toluene conversion of 94,1% was found at 900°C, using Ni/cordierite as catalyst. [2]

A study at Laboratoire des Matériaux, Surfaces et Procédés pour la Catalyse, at ECPM Strasbourg (France) showed the effect of the addition of CaO or $CaO - CaAl$ on olivine. The ability of the catalyst to transform tar molecules was investigated. Further, the olivine based catalyst is able to absorb carbon dioxide CO_2 which is formed during biomass gasification to favour hydrogen production. [8]

3 Materials and Methods

In this chapter preceding considerations to the test procedure are made. This includes the choice of reactions for tests with different bed materials, the description of equipment and the procedure. Additionally, the simulation tool COCO (Cape Open to Cape Open) simulation environment is explained.

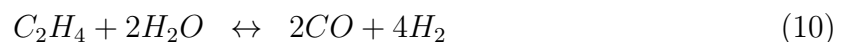
3.1 Reactions

Three reactions are chosen for catalytic tests on bed materials.

Water-Gas Shift Reaction The water-gas shift reaction (equation 9) is exothermic with a standard enthalpy of ($\Delta H = -41,5kJ/mol$). [8]. It is one of the reactions in the gasifier which can be easily recreated. According to its exothermic properties, the carbon monoxide conversion is better at lower temperatures than at gasifying operation temperatures of about 700°C to 900°C.



Steam Reforming of Ethene Steam reforming of ethene (equation 10) is an endothermic reaction. Therefore, the ethene conversion rate is higher at higher temperatures. Steam reforming of ethene was chosen to represent steam reforming of lighter hydrocarbons. As carbon monoxide CO is a product, this reaction will be followed by a water-gas shift reaction (equation 9), as long as steam is available.



Steam Reforming of Toluene Steam reforming of toluene (equation 11) is a strongly endothermic reaction. It has a standard enthalpy of ($\Delta H = 869,8kJ/mol$). [18] Thus, the toluene conversion rate is higher at higher temperatures. Toluene was chosen as a tar model compound and steam reforming of toluene represents steam reforming of heavier hydrocarbons. Like steam reforming of ethene, carbon monoxide CO is a product.

Therefore, this reaction will be followed by the water-gas shift reaction (equation 9), as long as steam is available.



3.2 Bed Materials

Four different bed materials were chosen. Beside calcium oxide, the bed materials are either used or fresh. In total seven different kinds of bed materials were investigated. Used bed material shows a calcium-rich layer. This layer strongly depends on the operation time of the bed material in the plant.

All bed materials were sieved and particles with a grain size between $400\mu m$ to $800\mu m$ are used for experiments. Following materials were investigated:

Olivine Olivine is currently in use as bed material in DFB gasification plants. It is a common, naturally occurring mineral containing magnesium, iron oxides and silica. [15] For the following catalytic investigations, fresh olivine and used olivine from the DFB gasification plant in Senden, Germany were collected.

Quartz Sand Fluidized bed combustion plants mainly use quartz sand as bed material. For the following catalytic investigations, fresh quartz sand and used quartz from the fluidized bed combustion plant in Heiligenkreuz, Austria were taken.

CarboHSP A research group in California, USA developed a new bed material called CarboHSP. Samples were provided for this research. New and used CarboHSP were investigated.

Calcium Oxide Calcium oxide CaO particles are not in use as bed material in fluidized bed gasification reactors, because of low abrasion resistance. Calcium oxide is used as reference, because the layer of used quartz sand or used olivine consists mainly of calcium. To prove catalytic effects, fresh calcium oxide particles were also part of the following catalytic investigations.

3.3 Equipment

The following equipments are used for the experiments.

Gas Bottles Pressurized gases are provided from gas bottles. Following gases will be used: carbon monoxide CO , ethane C_2H_4 and nitrogen N_2 .

Kinetic Test Rig The kinetic test rig includes the reactor, mass flow controllers, evaporating units and heating devices.

Cooler The product gas is cooled to room temperature. Water and toluene will condense and collected in a bottle.

Five Component Online Gas Analyzer (Rosemount, NGA 2000)

The gas analyzer can detect hydrogen H_2 , oxygen O_2 , carbon monoxide CO , carbon dioxide CO_2 and methane CH_4 . It measures volume percent.

Data Recording Computers Two computers for data recording are available. One computer records the output of mass flow controllers and the other computer records temperature and gas composition.

3.3.1 Description and Operation

Experiments were operated at the kinetic test rig at the laboratory of the Vienna University of Technology, see Figure 12. Core of the kinetic test rig is a plug flow reactor made of glass. Bed material is filled in the reactor and is fixed with quartz wool. Following, the reactor is heated to its operating temperature. Gas flows through the bed material particles, which act as catalyst. Electrical heating heat the reactor to its operation temperature. For the following experiments, three operation temperatures are selected 750°C, 800°C and 850°C.

Heating quartz sand causes a problem. At a temperature above 573°C, quartz changes its crystal structure. This leads to a light volume expansion, which breaks the glass reactor. While heating up, the reactor is shaken to move quartz sand particles and prevent destroying the glass reactor.

Gas is mixed by entering the reactor. The incoming gas contains steam, nitrogen N_2 as carrier gas for steam and according to requirements carbon monoxide CO , ethene C_2H_4 or evaporated toluene C_7H_8 .

The reactor is followed by a cooler, where steam and toluene condenses and get collected in a bottle. Before the product gas goes to the exhaust, a part stream goes to the five component online gas analyzer (Rosemount, NGA 2000). A steady gas composition for a duration of 5min is needed, to define an operation point. This values are used for further evaluations.

For safety reasons, a mobile gas detector is placed next to the test rig. It measures carbon monoxide CO , oxygen O_2 and hydrogen H_2 in the air and gives an alert, if a critical air composition occurs.

3.3.2 Adaptions

The kinetic test rig was constructed to insert only gaseous compounds in the reactor. Water is evaporated, before entering the reactive area. To insert toluene, a second inlet for fluid components has to be installed. It has to consist of an inlet pump, an mixing unit to add nitrogen N_2 which acts as a carrier gas and an evaporating unit.

Toluene is filled in a syringe and continuously forwarded to the nitrogen mixing unit and the evaporator by a syringe pump. Figure 13 shows the syringe pump used for experiments.

To mix toluene with nitrogen, a tee-connector is used. Toluene flows through a pipe with smaller diameter. This pipe is coaxially inserted in the bigger pipe. Nitrogen, which comes through the bigger pipe entrains the toluene. Figure 14 shows the tee-connector.

Toluene and nitrogen enter the evaporation unit. It consists of a contorted pipe, surrounded by heating bands. To prevent bigger heating losses, an insulation is added. Figure 15 shows the evaporating unit during construction.

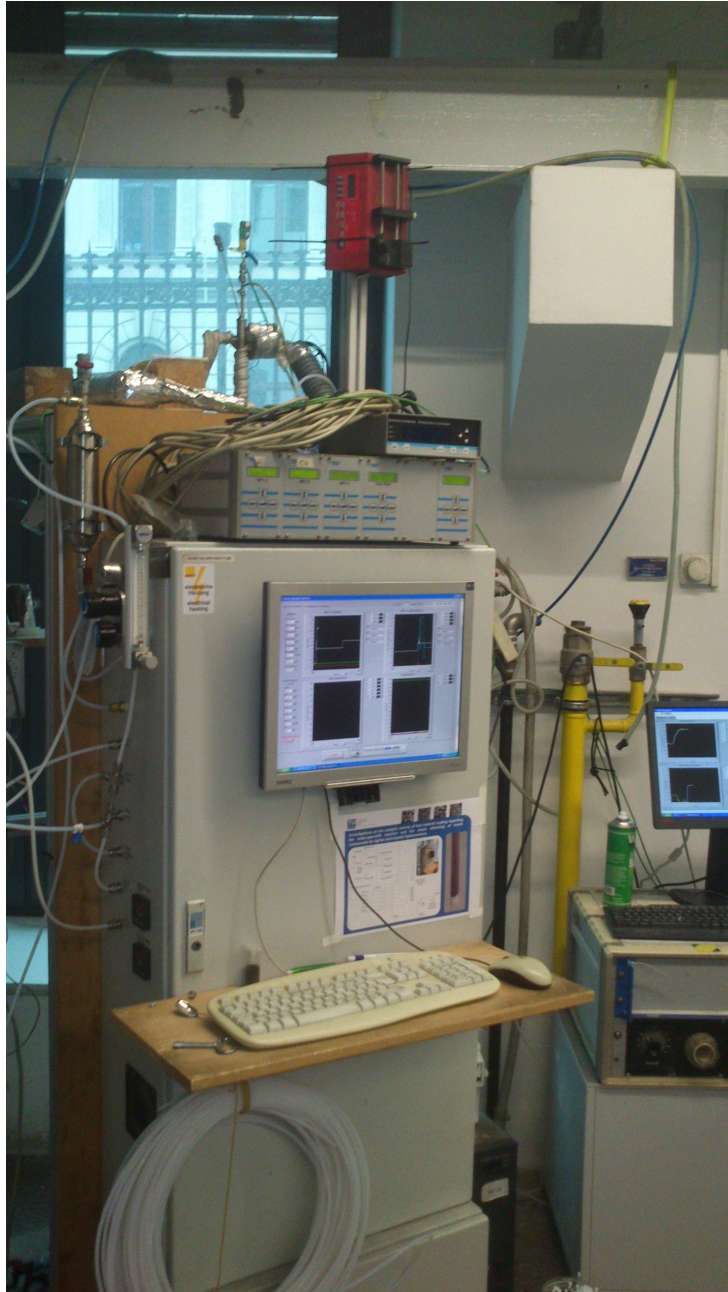


Figure 12: Test rig for experiments



Figure 13: Syringe pump for toluene injection



Figure 14: Tee-connector to mix nitrogen with toluene

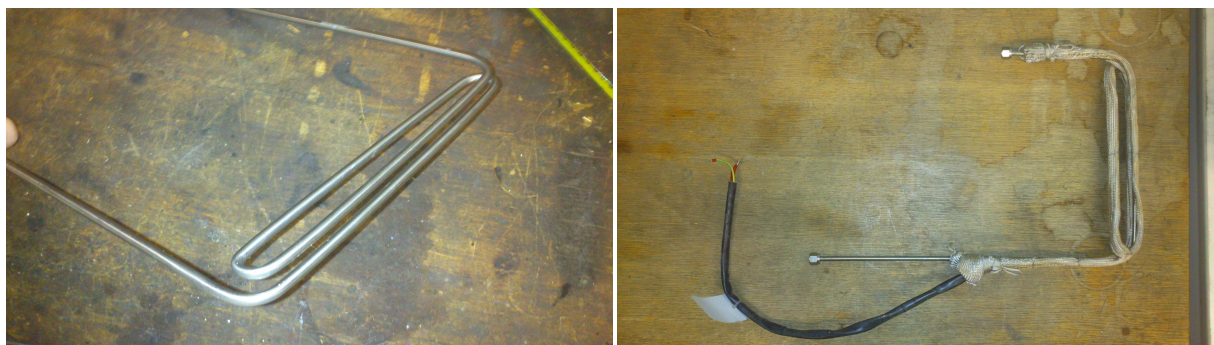


Figure 15: Constructing a toluene evaporator

3.4 Procedure

The reactor input consists of a steam-nitrogen mix and according to the reaction carbon monoxide CO , ethene C_2H_4 or a toluene-nitrogen mix. The flow rate of the components is set to the stoichiometric proportion of each reaction.

3.4.1 Flow Rate Calculation

For gas inputs (carbon monoxide CO , ethene C_2H_4 and nitrogen N_2), the flow rate has to be set in Nl/h (metric norm liters). Steam is set in g/h and toluene is set in ml/h. The mass flow rate \dot{m} is calculated according to equation 12 and the volume flow rate \dot{V} is calculated according to equation 13.

$$\dot{m} = \dot{n} \cdot M_i \quad (12)$$

$$\dot{V} = \frac{\dot{n} \cdot M_i}{\rho_i} \quad (13)$$

The base is the molar flow rate \dot{n} . Any value can be assumed, as long as the proportion to the other components is correct. Molar mass M_i and density ρ_i (at 20°C) is needed for calculations.

3.4.2 Water-Gas Shift Reaction

Corresponding to equation 9, mole values were calculated into volume flow rates and mass flow rates. The H_2O/CO ratio is 1/1. See table 1

Table 1: Calculated flow rates for the water-gas shift reaction

component	mole proportion	calculated flow rate	flow rate set for experiments
CO	1	15 Nl/h	15 Nl/h
H_2O	1	11,05 g/h	12,05 g/h
N_2	1,09	15 Nl/h	15 Nl/h

The flow rate for steam was set a little higher, then the stoichiometric value. This was done do be sure, that enough steam is in the reactor, since there is a possibility that water

condenses somewhere in the test rig. The volume flow rate for nitrogen N_2 was set to the same value like carbon monoxide CO .

3.4.3 Steam Reforming of Ethene

Corresponding to equation 10, mole values were calculated into volume flow rates and mass flow rates. The H_2O/C_2H_4 ratio is 2/1. See table 2

Table 2: Calculated flow rates for steam reforming of ethene

component	mole proportion	calculated flow rate	flow rate set for experiments
C_2H_4	1	11 Nl/h	11 Nl/h
H_2O	2	16,65 g/h	18 g/h
N_2	1,06	11 Nl/h	11 Nl/h

As done at the water-gas shift experiment, the flow rate for steam was set a little higher, then the stoichiometric value. This was done do prevent possible steam losses due to condensations somewhere in the test rig. The volume flow rate for nitrogen N_2 was set to the same value like carbon monoxide CO .

3.4.4 Steam Reforming of Toluene

Corresponding to equation 11, mole values were calculated into volume flow rates and mass flow rates. The water/toluene ratio (H_2O/C_7H_8 ratio) is 7/1. See table 3

Table 3: Calculated flow rates for steam reforming of toluene

component	mole proportion	calculated flow rate
C_7H_8	1	21,18 ml/h
H_2O	7	25,2 g/h
N_2 (carrier gas steam)	0,34	1,5 Nl/h
N_2 (carrier gas toluene)	0,23	1 Nl/h

Regarding the possibility, that water-gas shift reaction occurs in addition, a second experiment setup with a higher steam rate was calculated. Calculations in table ref bases on equation 14, which includes the water-gas shift reaction into steam reforming of toluene. The water/toluene ratio is 14/1 instead of 7/1.

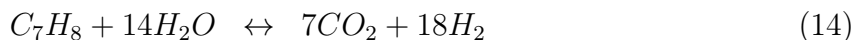


Table 4: Calculated flow rates for steam reforming of toluene combined with the water-gas shift reaction

component	mole proportion	calculated flow rate
C_7H_8	1	10,59 ml/h
H_2O	14	25,2 g/h
N_2 (carrier gas steam)	0,68	1,5 NI/h
N_2 (carrier gas toluene)	0,45	1 NI/h

Therefore, steam reforming of toluene test were conducted in two modes. First mode is a water/toluene ratio of 7/1 and second mode is a water/toluene ratio of 14/1.

Two carrier gas streams are needed. In total, the flow rate is 2,5NI/h. This is lower than the carrier gas flow rate at the other reactions (water-gas shift reaction and steam reforming of ethene). Since almost no hydrogen was detected at first test runs, the carrier gas streams were reduced to a minimum. The volume flow controllers can't set a flow rate below 1NI/h. This value is still enough to entrain the evaporated compounds.

In contrast to the other reactions, the exact flow rate values (for steam and toluene) were used in the experiment. At this experiment, the condensate of water and toluene was measured. Thus, conversion rate calculations were tried to kept as simple as possible.

At this experiment, only fresh olivine, used olivine, used quartz sand and calcium oxide are investigated. Toluene tests required a lot of time. Therefore, fresh and used CarboHSP and fresh quartz sand are not examined, because these materials are not in focus for this test.

3.4.5 Flow Sheet

After adaptations for toluene injection, an already existing flow sheet of the test rig and its compounds was modified. Figure 16 shows the actual version.

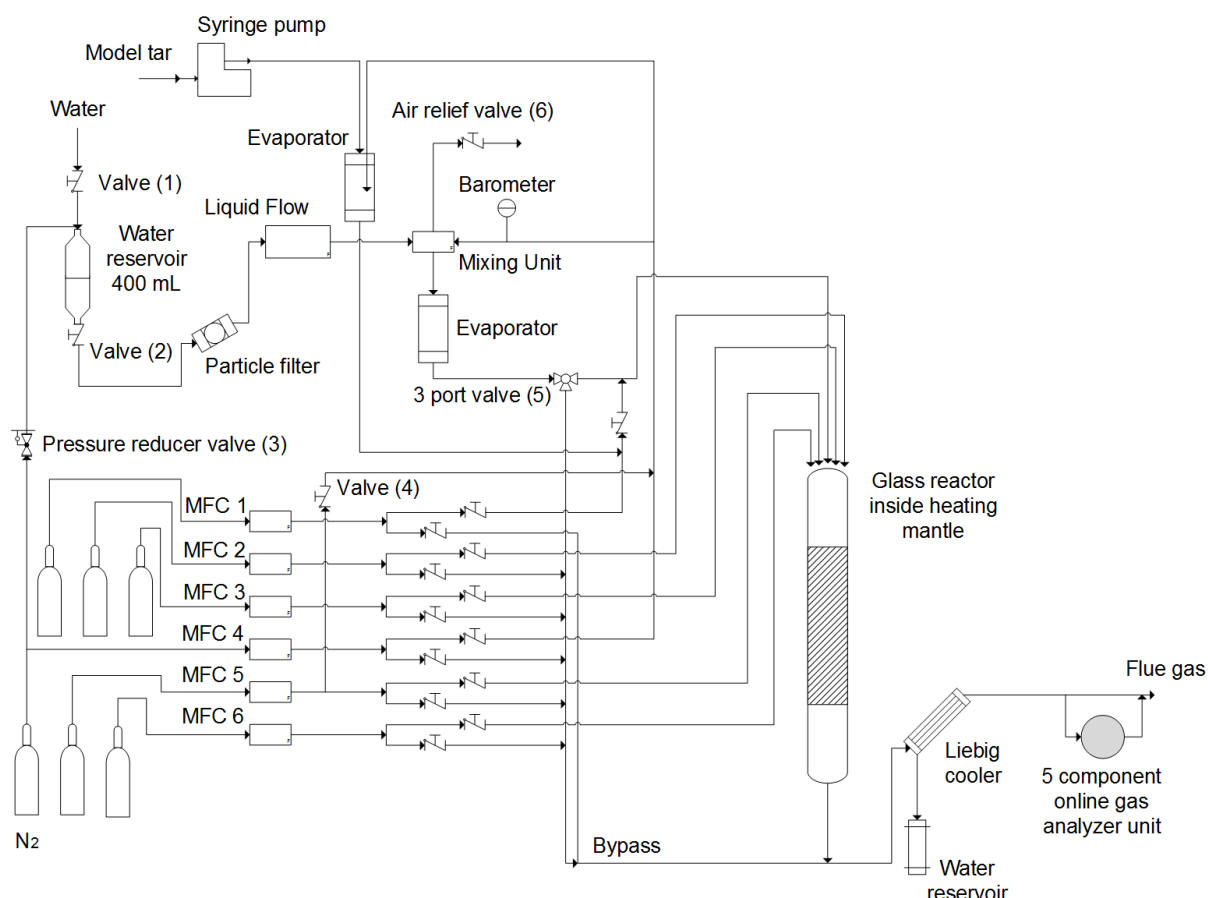


Figure 16: Actual flow sheet of the test rig and its compounds (Vienna University of Technology)

Six mass flow controllers for six different gases are available. For the following experiments, only three are used. The volume flow has to be set. The test rig has an liquid flow controller for steam, where a mass flow can be set. The flow rate of toluene is controlled with the syringe pump.

After the mass flow controllers, gases can be led directly into the reactor, or through a bypass. Starting an experiment, gases flow through the bypass first to swamp air out of the tubes. If a steady gas composition is measured, valves can be switched to lead gas

streams into the reactor.

After the reactor, water and toluene get condensed and the gas composition is measured.

3.5 Simulation

To have a better understanding how reactions emerge, a simulation of the reactions is done with Cape Open to Cape Open (COCO) simulation environment. With this free software, simple flow sheets can be designed. In addition, reactions can be calculated. The figures 17-19 show the flow sheet of the water-gas shift reaction, steam reforming of ethene and steam reforming of toluene. No carrier gas stream is added, to keep calculations and results simple.

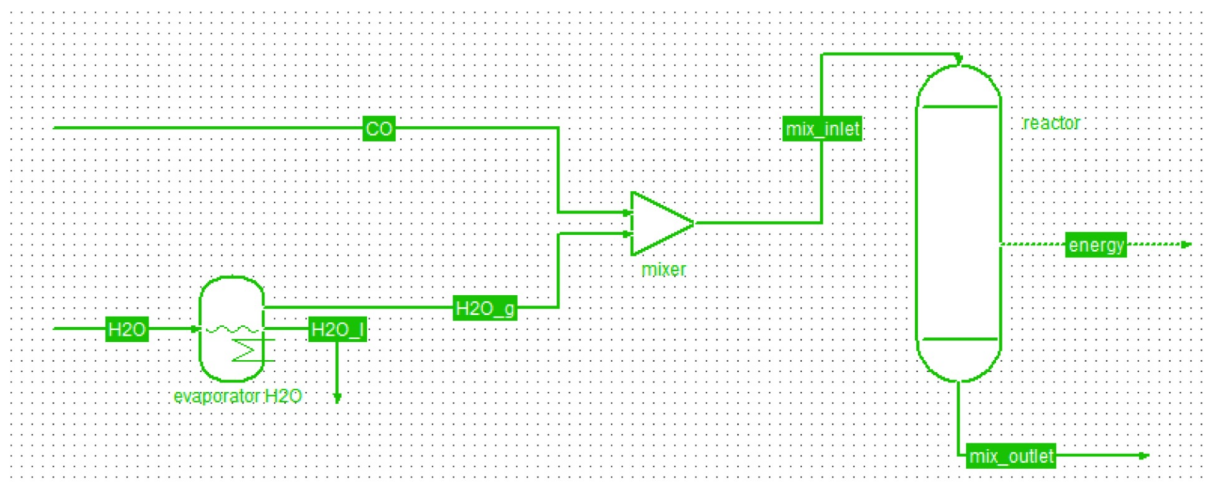


Figure 17: Flow sheet of the water-gas shift reaction in the COCO simulation environment

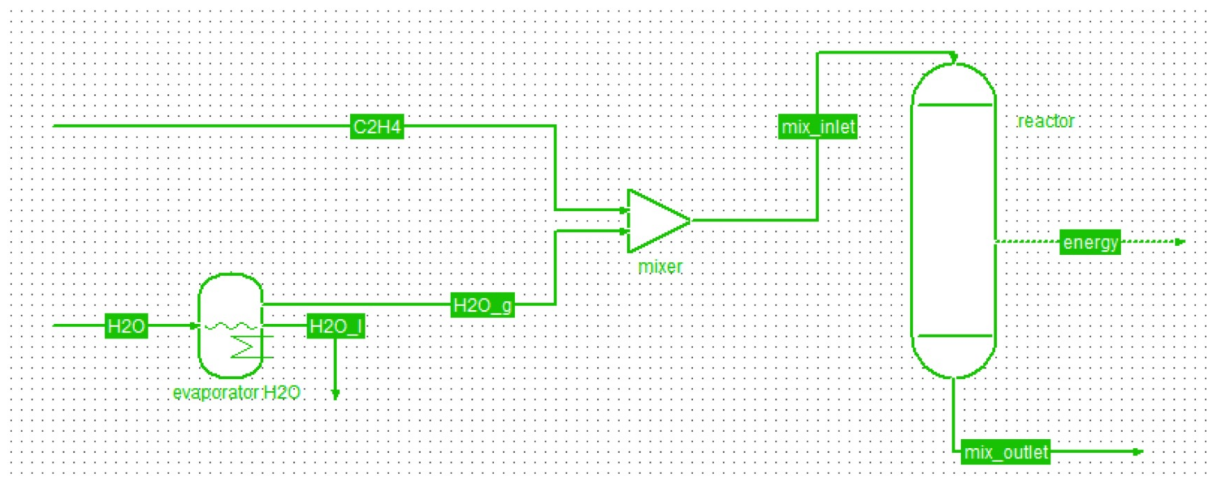


Figure 18: Flow sheet of steam reforming of ethene in the COCO simulation environment

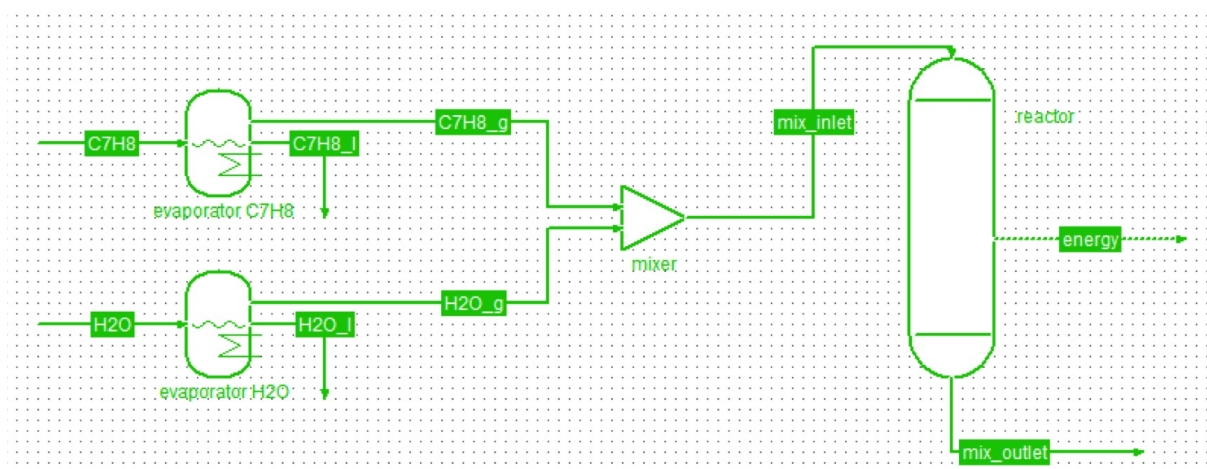


Figure 19: Flow sheet of steam reforming of toluene in the COCO simulation environment

4 Results

Following results are classified by the type of reaction. First, results of the COCO simulation environment are shown and then the output of the five-component-gas-analyzer is presented. The following results are presented in diagrams. Since multiple tests were executed, only the results of the most promising experiments are shown in this chapter. Numerical results of all tests are presented in the appendix and structured in tables. In chapter 5, results will be compared and discussed.

4.1 Water-Gas Shift Reaction

4.1.1 Simulation Results

Since the water-gas shift reaction is exothermic, the simulation results show a lower carbon monoxide conversion at higher temperatures (see figure 20).

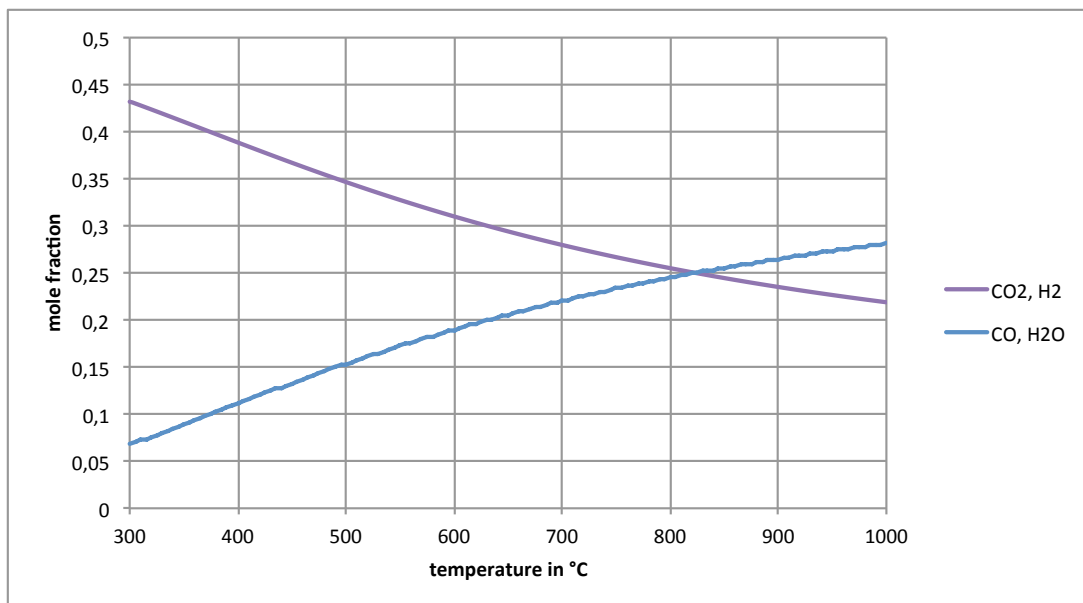


Figure 20: COCO-Simulation result of the water-gas shift reaction

4.1.2 Experimental Results

Figures 21-23 show the measured volumetric composition out of all gaseous components at 20°C in the product gas flow, including nitrogen. Every diagram illustrates a temperature. On the x-axis, different bed materials are listed.

In general, a higher hydrogen and carbon dioxide amount occurs at higher temperatures. Diagrams show also, that the use of calcium oxide as a catalyst leads to the best conversion rate.

Figure 24 shows the hydrogen production by temperature in molar proportion. Since water was not measured the molar proportion is out of carbon monoxide, carbon dioxide and hydrogen. The equilibrium hydrogen production by temperature is calculated with results from COCO simulation environment.

Best hydrogen production takes place with calcium oxide as catalyst, followed by used olivine, used quartz sand and fresh olivine. Fresh CarboHSP, used CarboHSP and fresh quartz sand lead to almost no hydrogen production. The equilibrium of hydrogen production according to COCO simulation environment is slightly lower than hydrogen production with calcium oxide as catalyst.

Figure 25 shows the carbon dioxide production by temperature in molar proportion. The equilibrium carbon dioxide production by temperature is calculated with results from COCO simulation environment. This diagram is similar to the hydrogen production rate. Calcium oxide as catalyst leads to best carbon dioxide generation, followed by used olivine and fresh olivine.

Figure 26 shows the carbon monoxide conversion rate X_{CO} , which was calculated according equation 15.

$$X_{CO} = \frac{[CO]_{in} - [CO]_{out}}{[CO]_{in}} \quad (15)$$

Thereby, $[CO]_{in}$ is the molar concentration of carbon monoxide entering the reactor and $[CO]_{out}$ the molar concentration of carbon monoxide leaving the reactor.

Similar to figure 24 and figure 25, calcium oxide as catalyst shows best carbon monoxide conversion rates, followed by used olivine, fresh olivine and quartz sand (Figure 26). In general, the equilibrium conversion rate calculated by COCO simulation environment is lower than conversion rates produced by calcium oxide as catalyst.

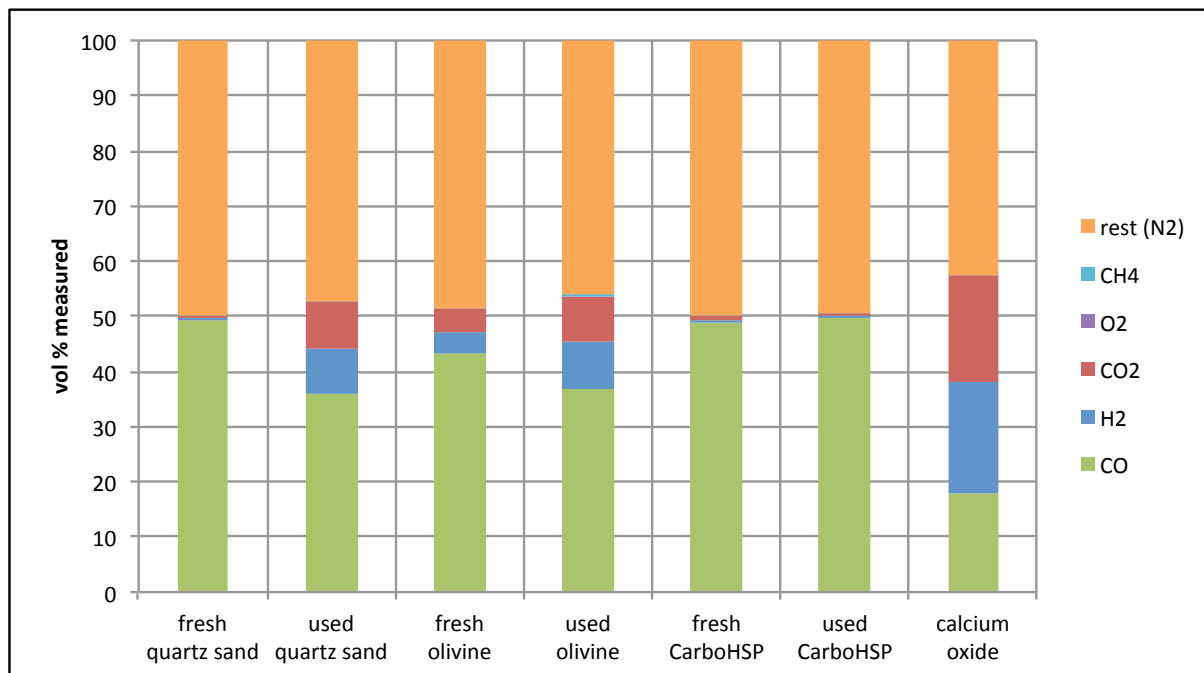


Figure 21: Volumetric composition at 750°C reactor temperature

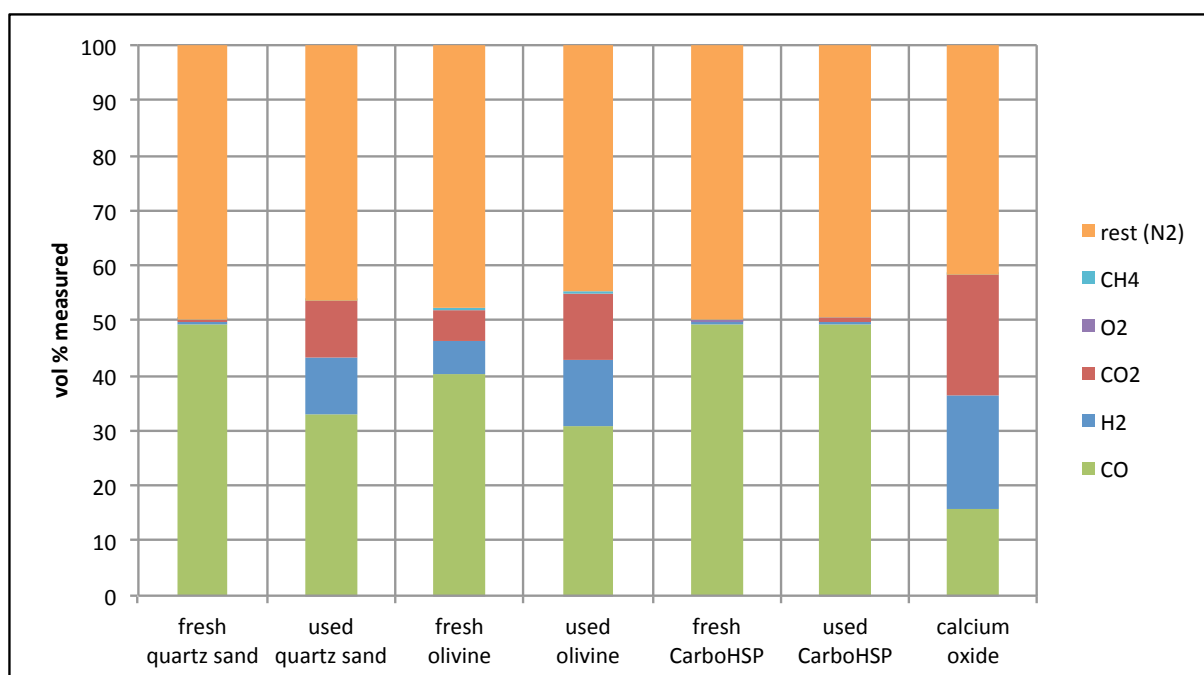


Figure 22: Volumetric composition at 800°C reactor temperature

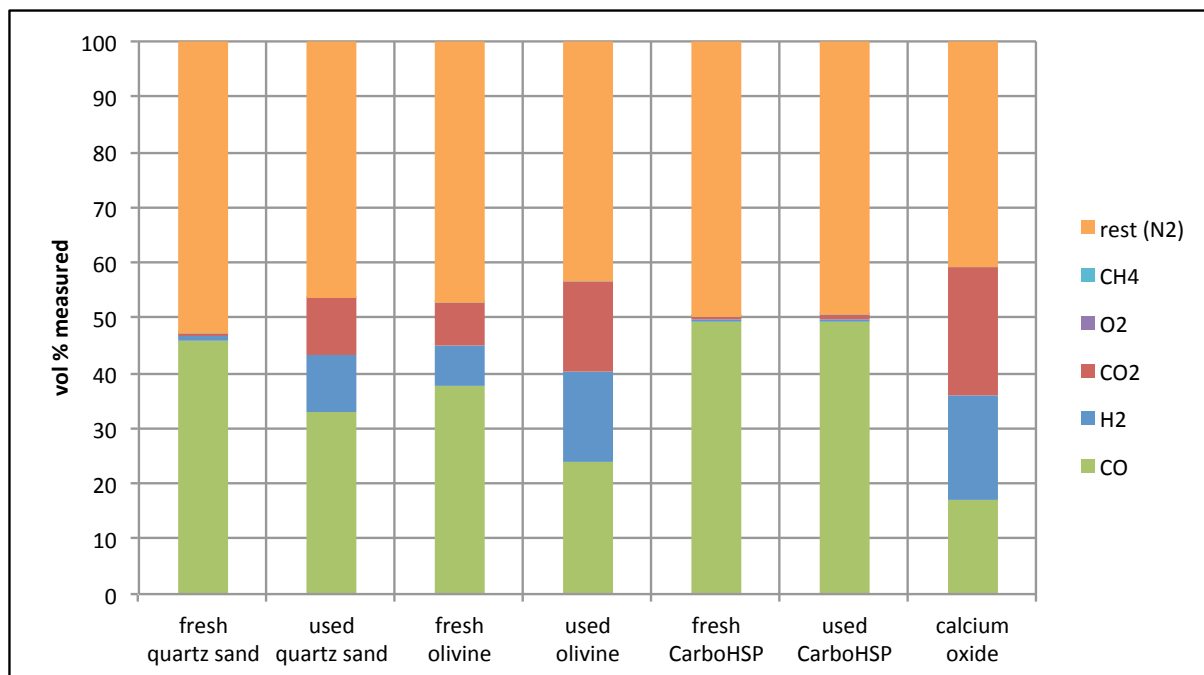


Figure 23: Volumetric composition at 850°C reactor temperature

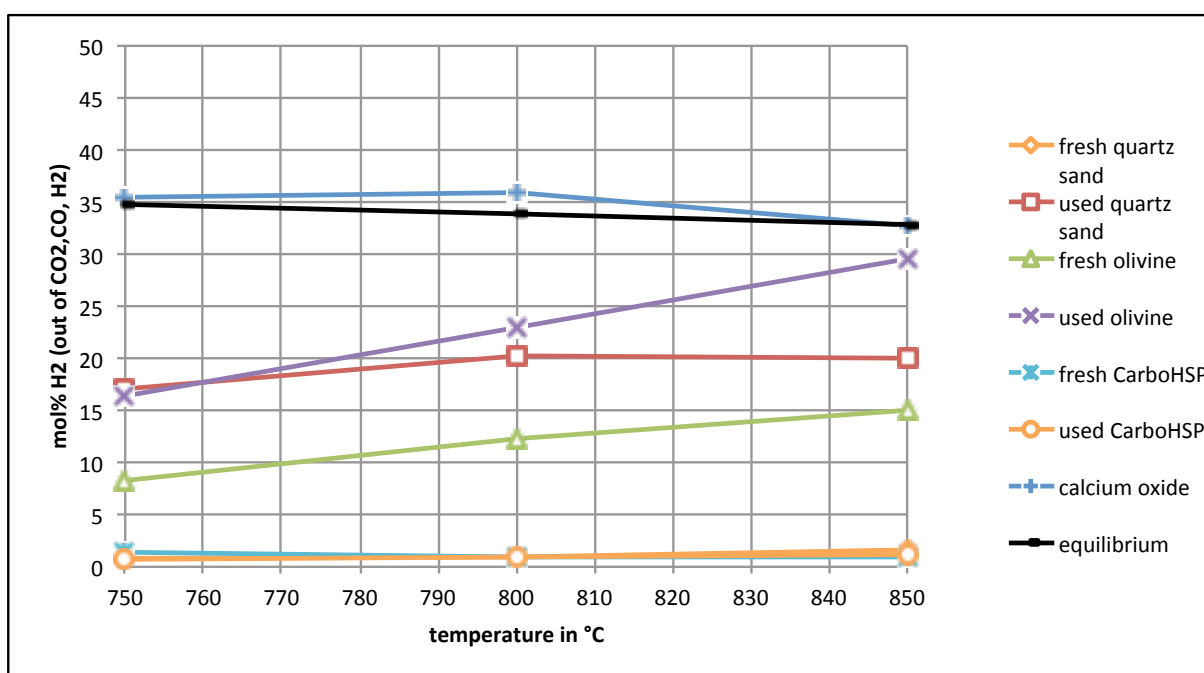


Figure 24: Molar proportion of hydrogen in the product gas

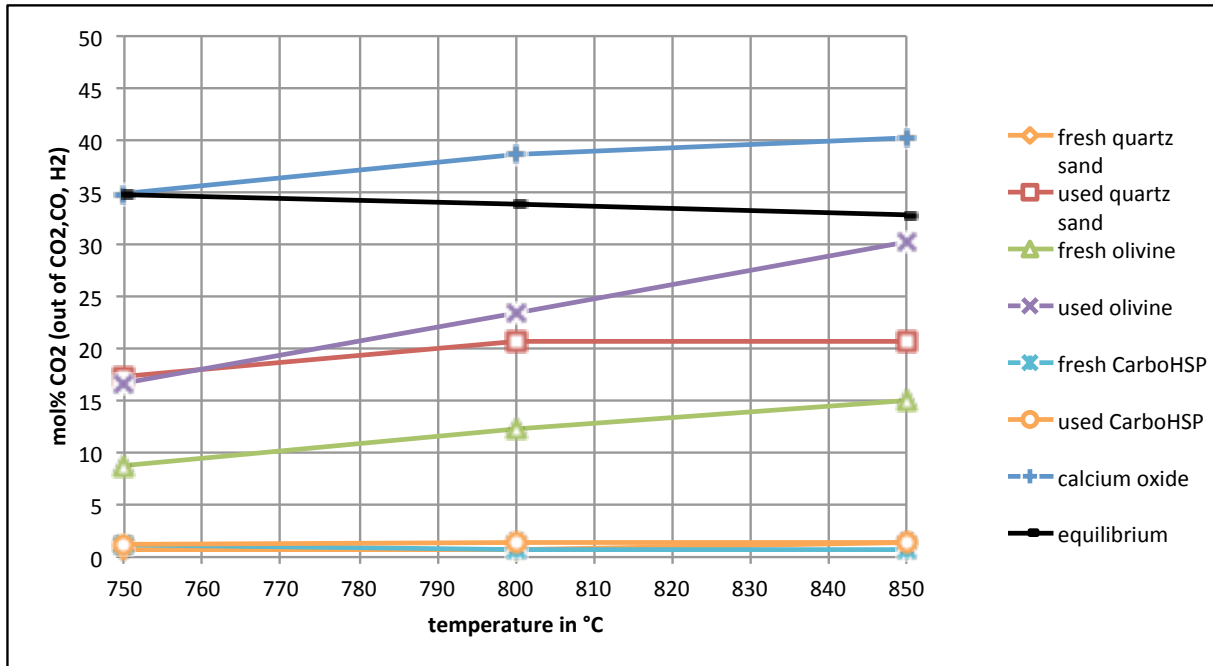


Figure 25: Molar proportion of carbon dioxide in the product gas

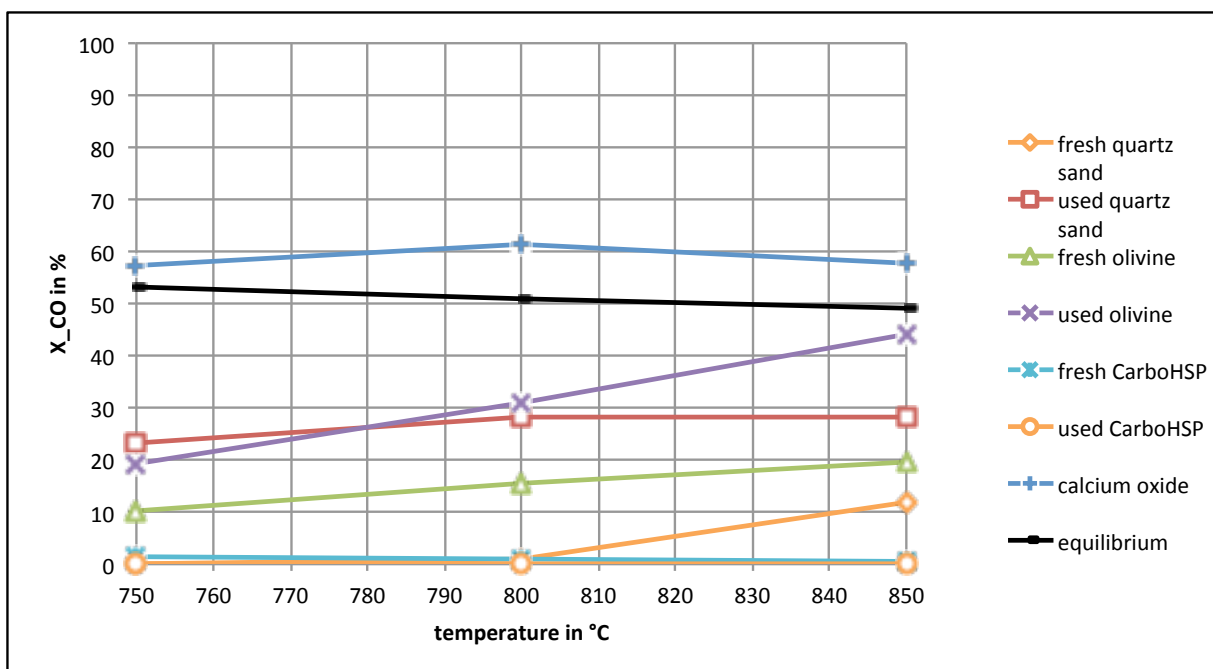


Figure 26: Carbon monoxide conversion rate

4.2 Steam Reforming of Ethene

4.2.1 Simulation Results

Figure 27 shows simulation results of steam reforming of ethene combined with the water-gas shift reaction. Since steam reforming of ethene is strongly endothermic and the water gas shift reaction slightly exothermic, higher ethene conversion occurs at higher temperatures. Reaction results at temperatures higher than 700°C are almost independent from temperature.

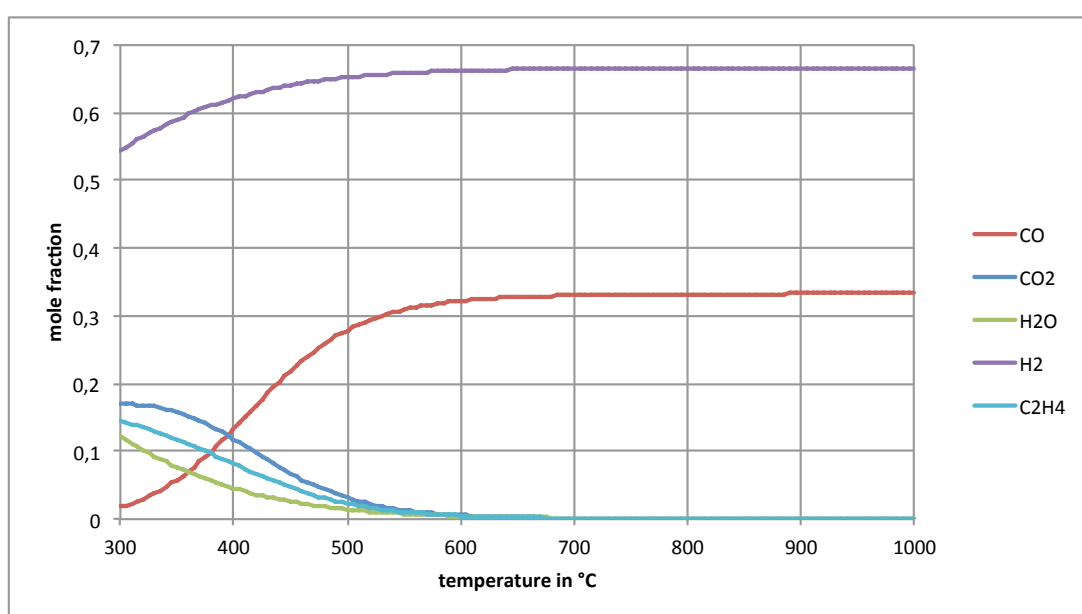


Figure 27: COCO-Simulation results of steam reforming of ethene combined with the water-gas shift reaction

4.2.2 Experimental Results

Figures 28-30 show the measured volumetric composition out of all gaseous components at 20°C in the product gas flow, including nitrogen. Every diagram illustrates a temperature. On the x-axis, different bed materials are listed.

In general, a higher hydrogen and carbon dioxide amount occurs at higher temperatures. These diagrams also show, that the use of calcium oxide as a catalyst leads to the best conversion rate.

Figure 31 shows the hydrogen production by temperature in volume proportion. Since water was not measured the volume proportion is out of all gaseous components at 20°C in the product gas flow, including nitrogen.

Best hydrogen production takes place with calcium oxide as catalyst, followed by used olivine, used quartz sand and fresh olivine. Fresh CarboHSP, used CarboHSP and fresh quartz sand lead to almost no hydrogen production. Hydrogen production strongly increases at higher temperatures.

Calcium oxide as catalyst leads to best carbon dioxide generation. Used olivine, used quartz sand and fresh olivine as catalysts lead to better carbon dioxide production than fresh CarboHSP, used CarboHSP and fresh quartz sand, which show almost no carbon dioxide generation. Carbon dioxide production increases at higher temperatures.

A transformation of the experimental results into molar proportion was not possible, because the gas analyzer doesn't measure ethene and no volume flow of the product gas was measured. COCO simulation environment results are displayed in molar proportion excluding nitrogen. Therefore, no equilibrium line can be drawn in figure 31

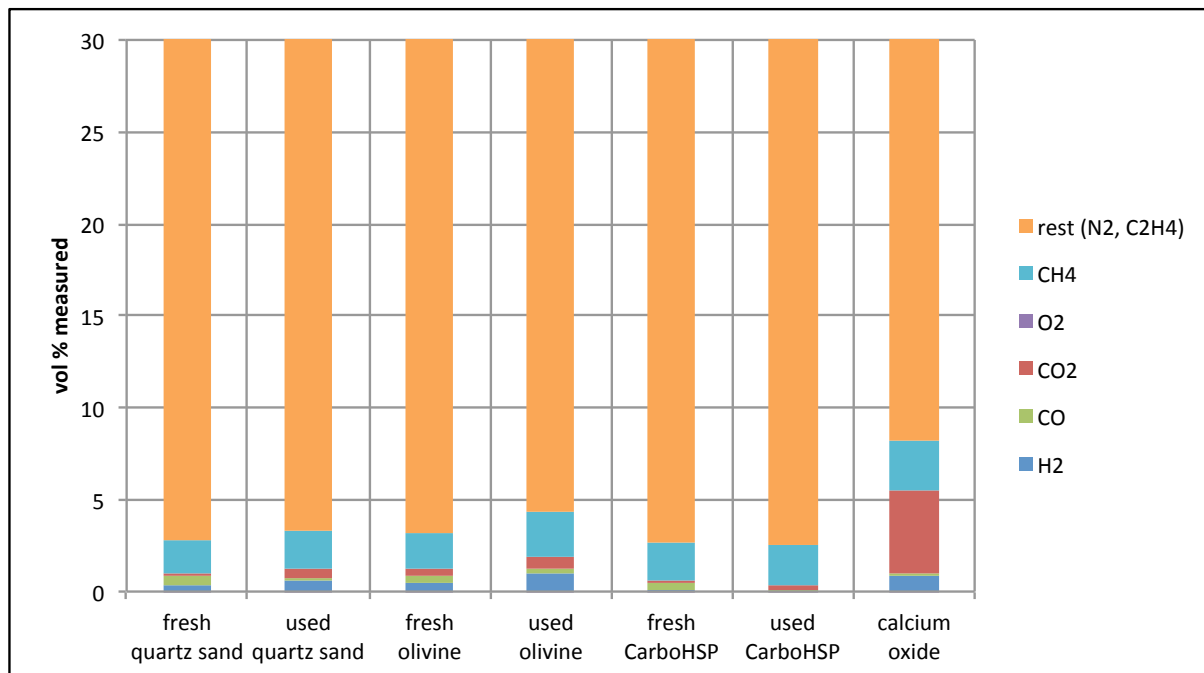


Figure 28: Volumetric composition at 750°C reactor temperature

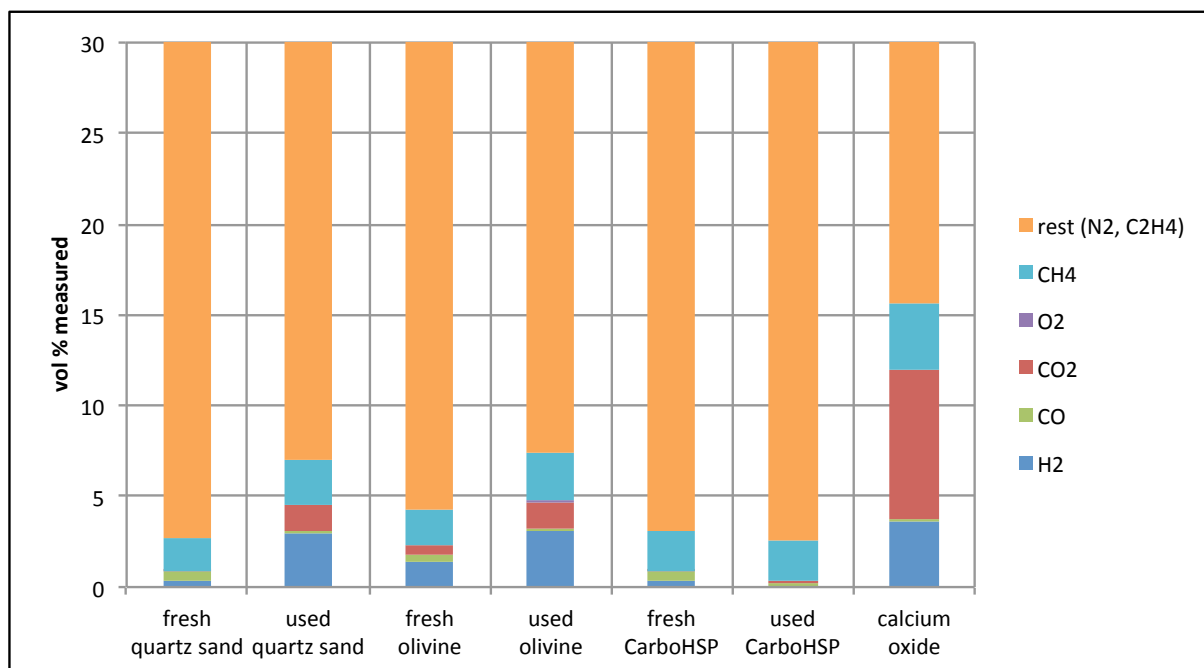


Figure 29: Volumetric composition at 800°C reactor temperature

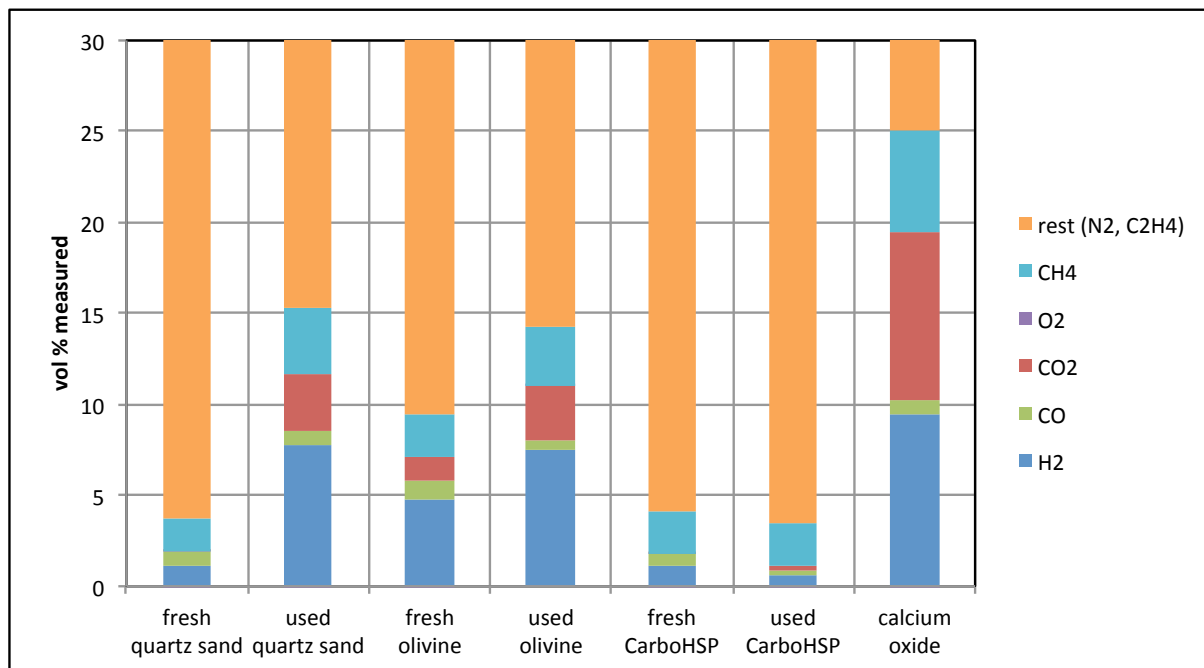


Figure 30: Volumetric composition at 850°C reactor temperature

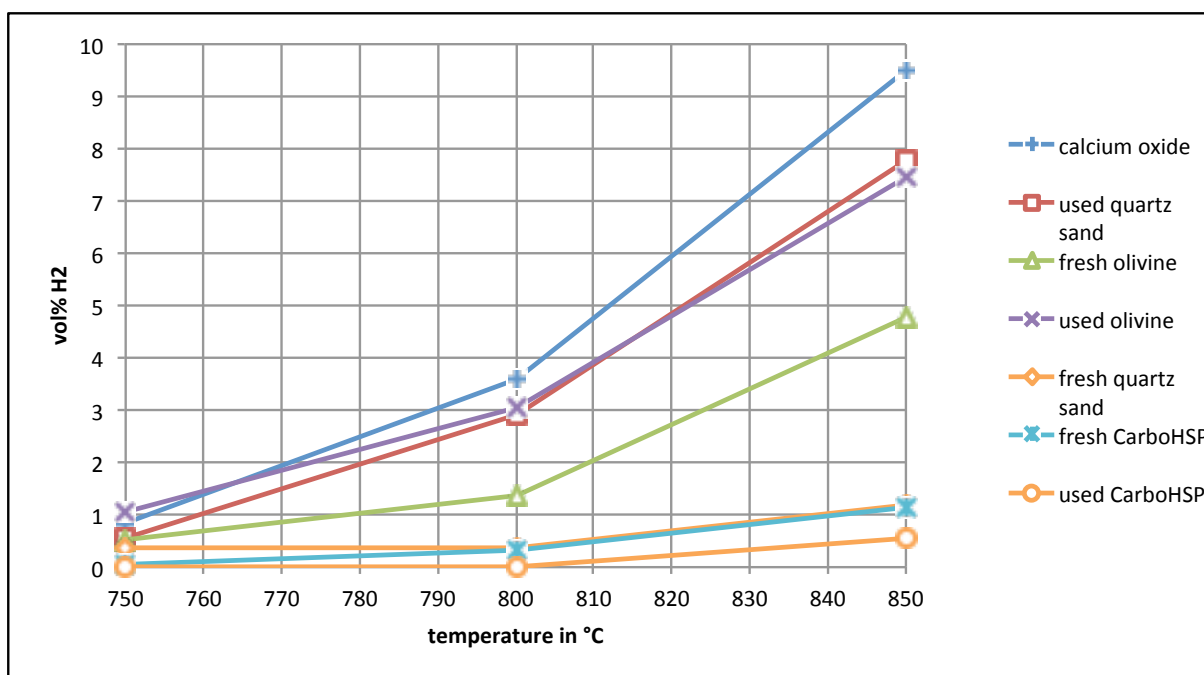


Figure 31: Volumetric proportion of hydrogen in the product gas

4.3 Steam Reforming of Toluene

4.3.1 Simulation Results

Figure 32 shows simulation results of steam reforming of toluene combined with the water-gas shift reaction. The molar water/toluene ratio is 7/1. Since steam reforming of toluene is strongly endothermic and the water gas shift reaction slightly exothermic, higher ethene conversion occurs at higher temperatures. Reaction results at temperatures higher than 700°C are almost independent from temperature.

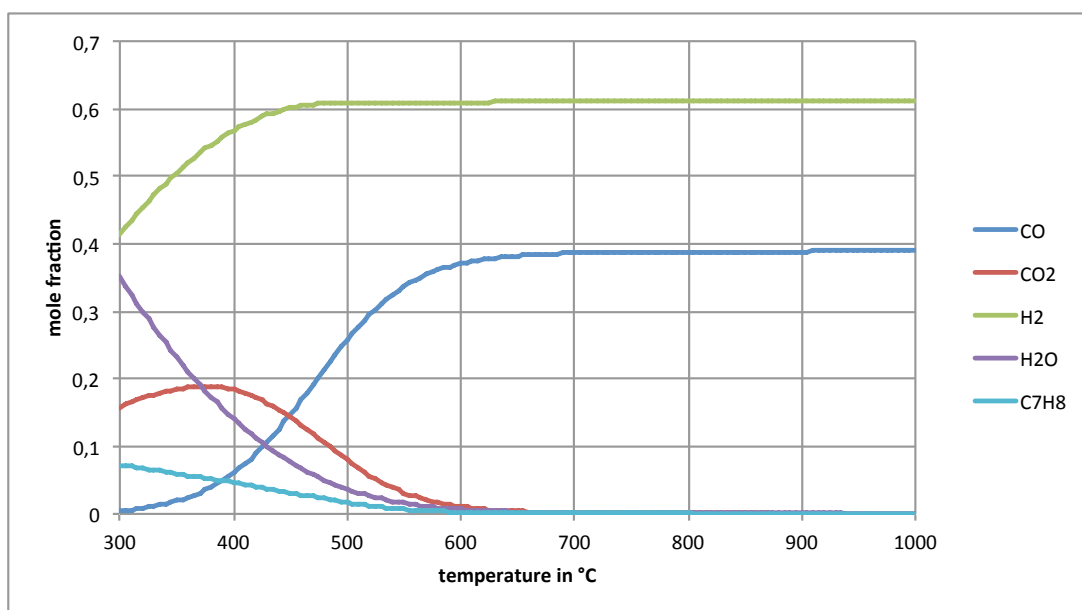


Figure 32: COCO-Simulation results of steam reforming of toluene combined with the water-gas shift reaction at a molar water/toluene ratio of 7/1

Figure 33 shows simulation results of steam reforming of toluene combined with the water-gas shift reaction with a molar water/toluene ratio of 14/1. At higher temperatures, hydrogen production goes down and the water content in the product rises.

In this diagram, starting at 450°C, the curve of water is congruent with the curve of carbon monoxide.

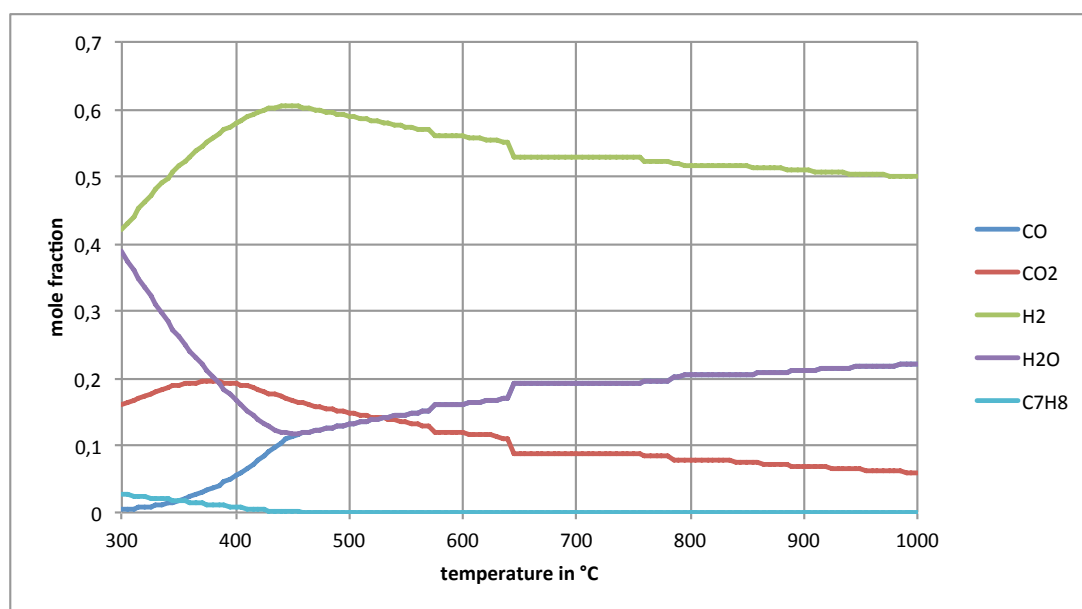


Figure 33: -COCO-Simulation results of steam reforming of toluene combined with the water-gas shift reaction at a molar water/toluene ratio of 14/1

4.3.2 Experimental Results

Figures 34-39 show the measured volumetric composition out of all gaseous components at 20°C in the product gas flow, including nitrogen. Every diagram illustrates a temperature and a water/toluene ratio. On the x-axis, different bed materials are listed.

In general, a higher hydrogen and carbon dioxide amount occurs at higher temperatures. Diagrams also show, that the use of calcium oxide as a catalyst leads to the best conversion rate. The water/toluene ratio of 14/1 leads to a slightly lower hydrogen and carbon dioxide production than the water/toluene ratio of 7/1.

Figure 40 (water/toluene ratio 7/1) and figure 41 (water/toluene ratio 14/1) show the hydrogen production by temperature in volume proportion. Water and toluene was measured, but the results are insufficient for further calculations. This problem will be exemplified in chapter 5. Therefore, the volume proportion is only out of all gaseous components at 20°C in the product gas flow, including nitrogen.

Best hydrogen production takes place with calcium oxide as catalyst, followed by used

olivine, used quartz sand and fresh olivine. Only a small difference is seen at different water/toluene ratios. The water/toluene ratio of 14/1 leads to a insignificant lower hydrogen production.

A transformation of the experimental results into molar proportion was not possible, because no volume flow of the product gas was measured and the results of measured water and toluene were insufficient, as mentioned before. COCO simulation environment results are displayed in molar proportion excluding nitrogen. Therefore, no equilibrium line can be drawn in figure 40 and figure 41

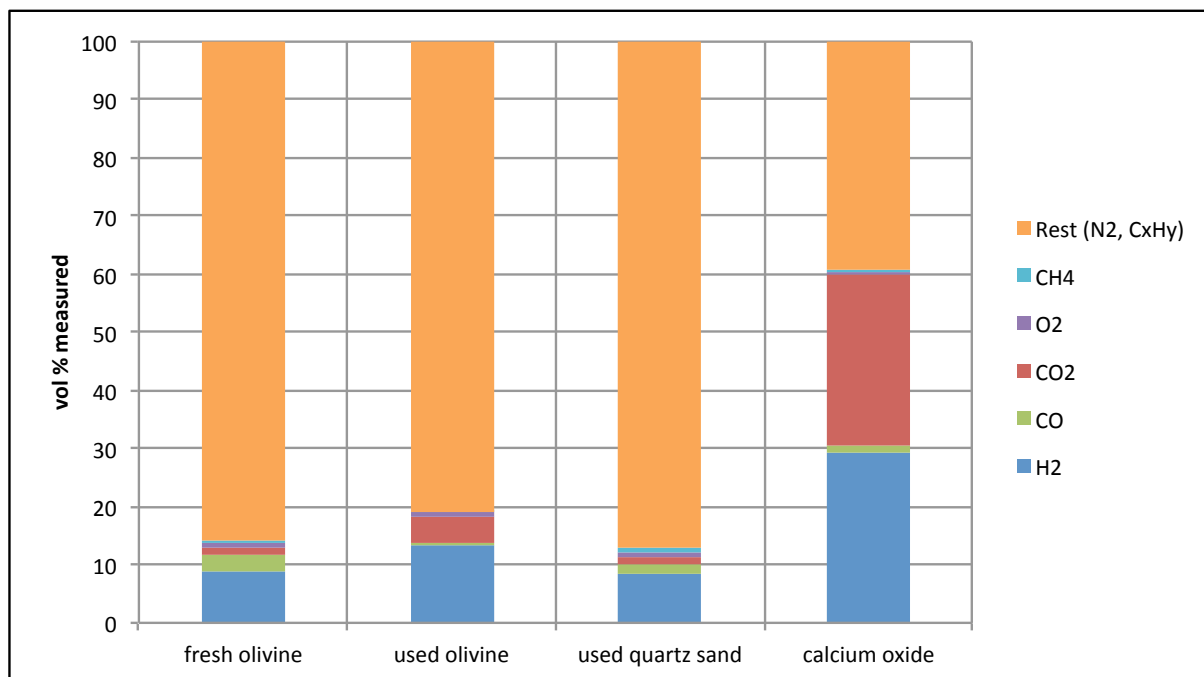


Figure 34: Volumetric composition at 750°C reactor temperature and 7/1 water/toluene ratio

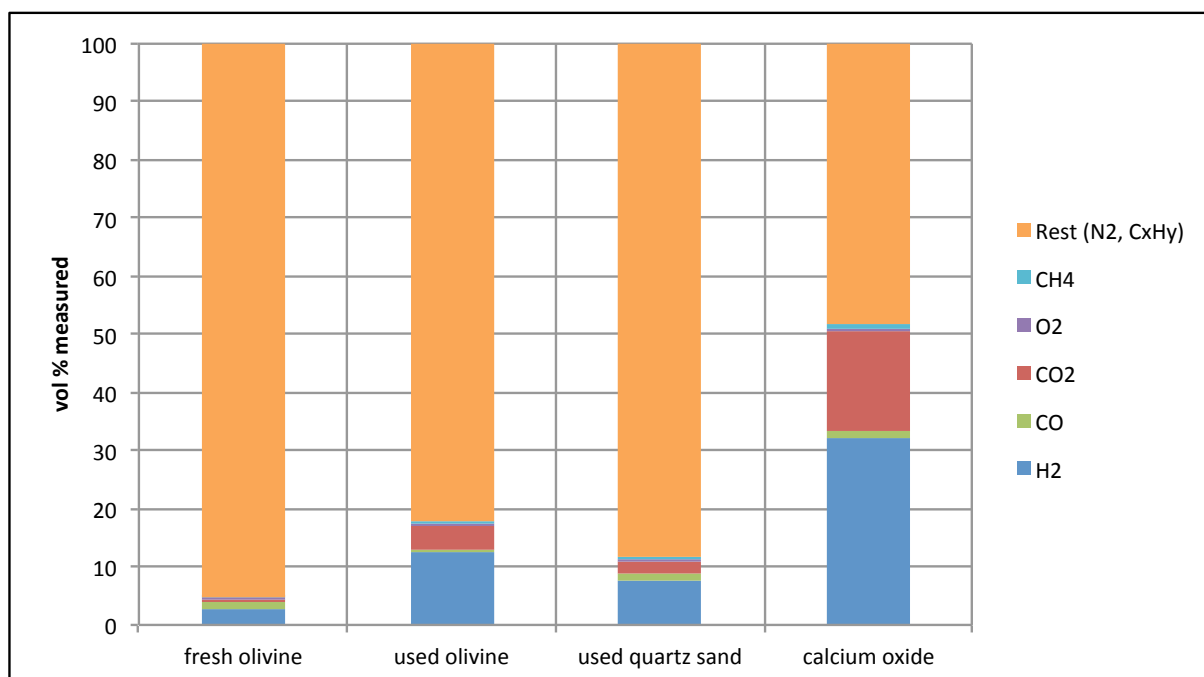


Figure 35: Volumetric composition at 750°C reactor temperature and 14/1 water/toluene ratio

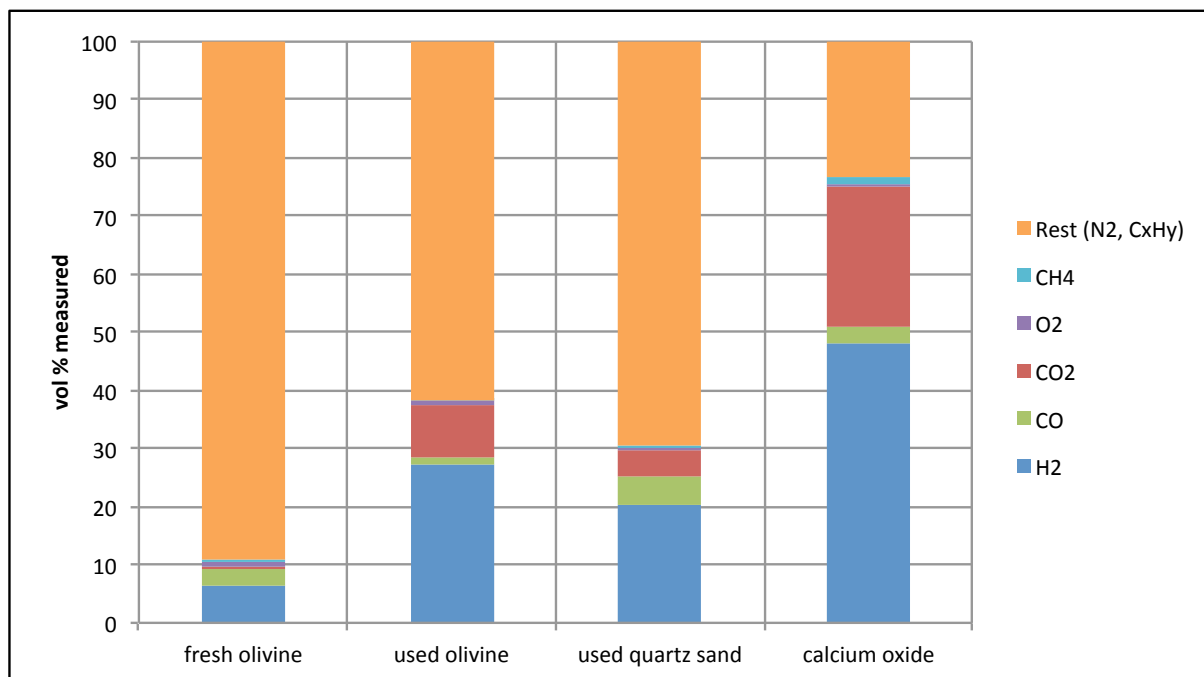


Figure 36: Volumetric composition at 800°C reactor temperature and 7/1 water/toluene ratio

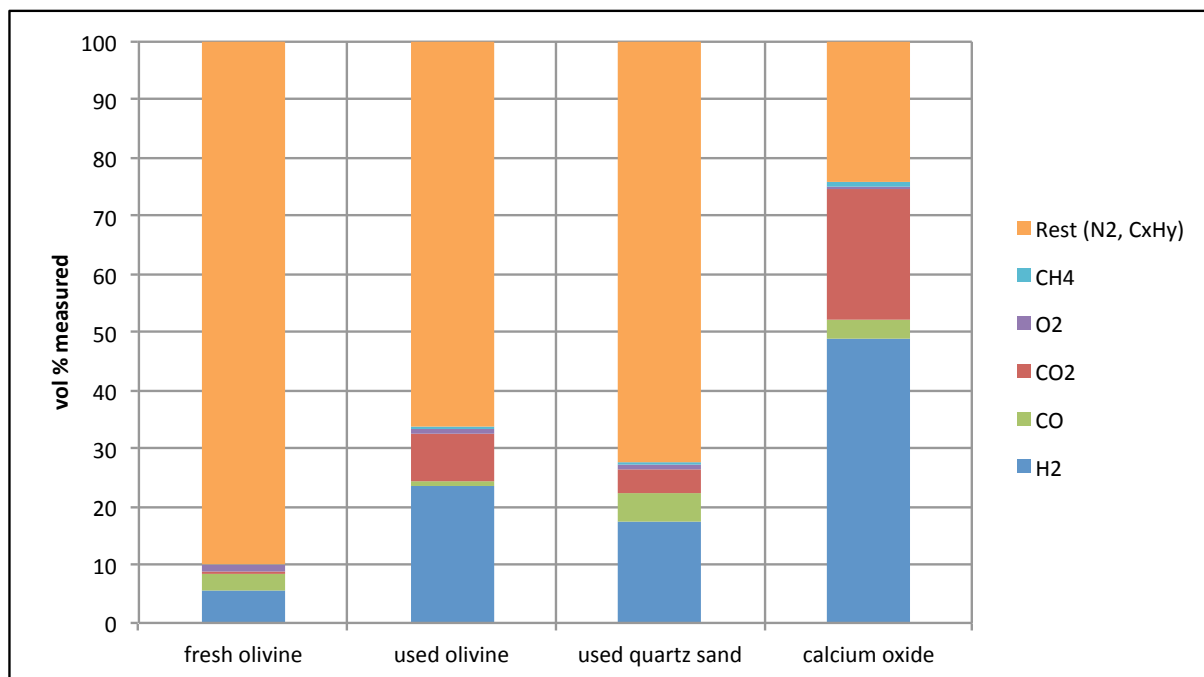


Figure 37: Volumetric composition at 800°C reactor temperature and 14/1 water/toluene ratio

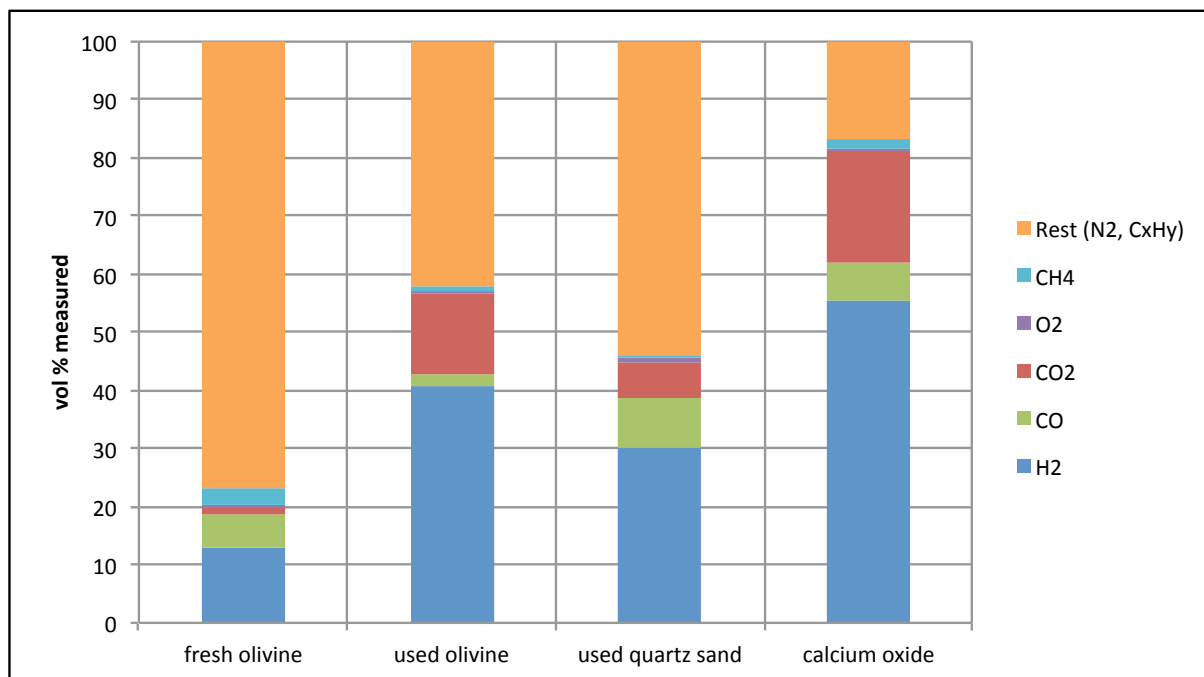


Figure 38: Volumetric composition at 850°C reactor temperature and 7/1 water/toluene ratio

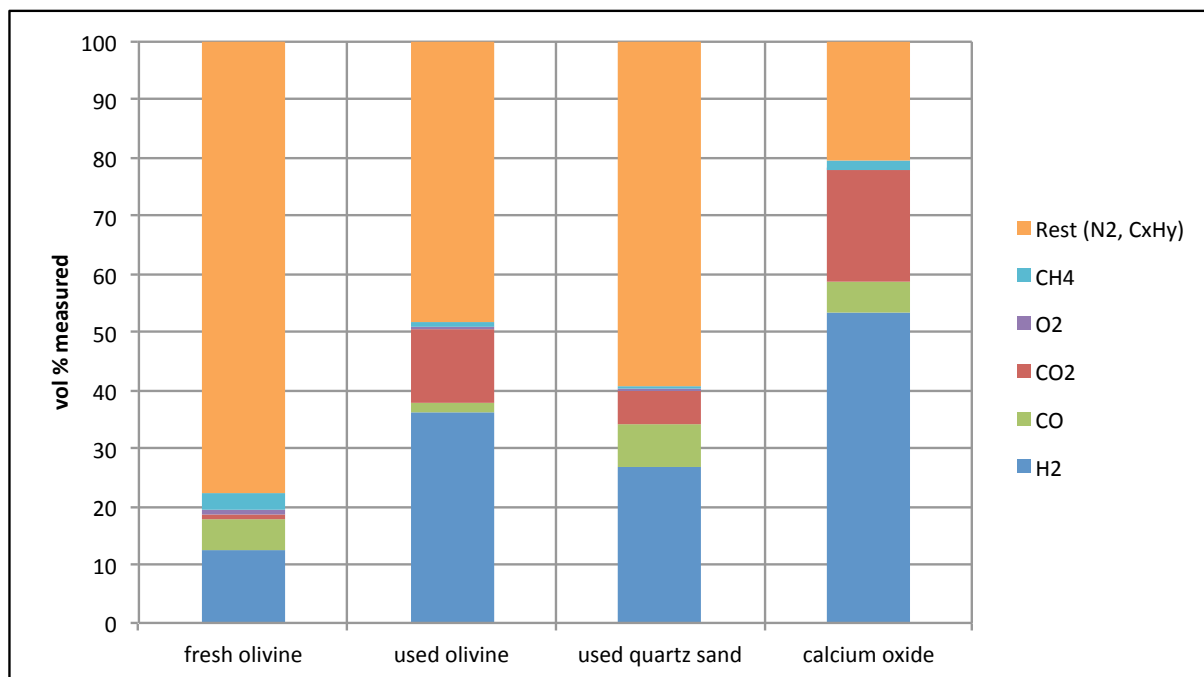


Figure 39: Volumetric composition at 850°C reactor temperature and 14/1 water/toluene ratio

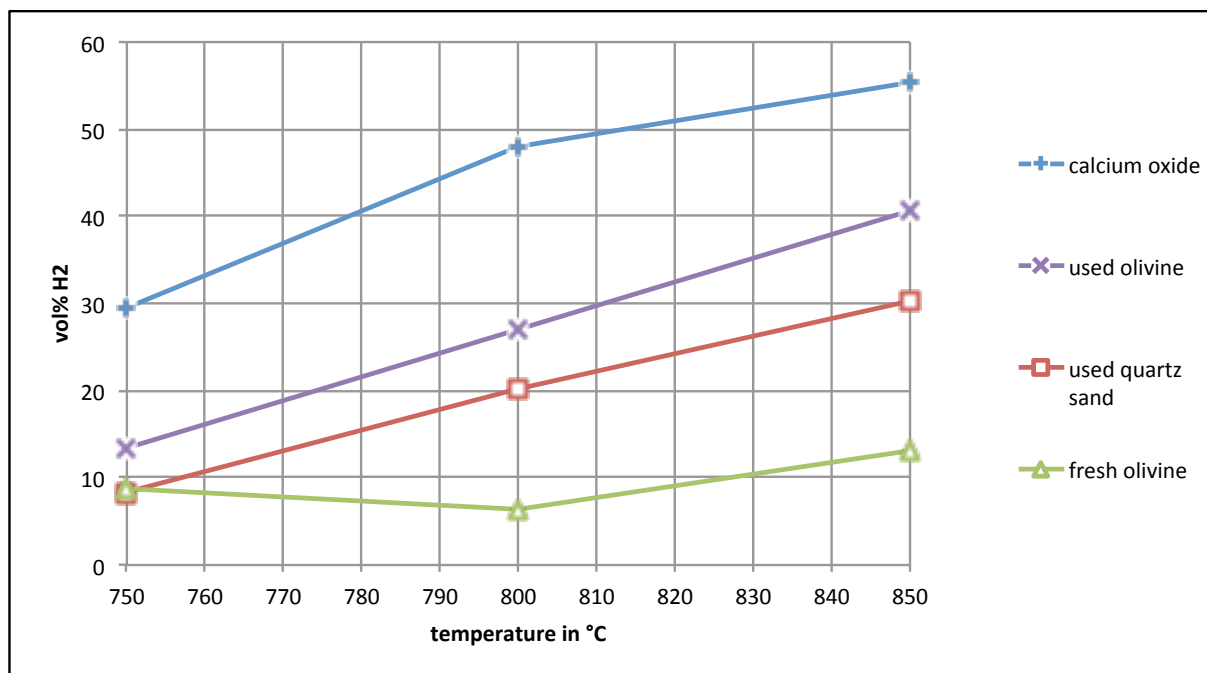


Figure 40: Volumetric proportion of hydrogen in the product gas at a water/toluene ratio of 7/1

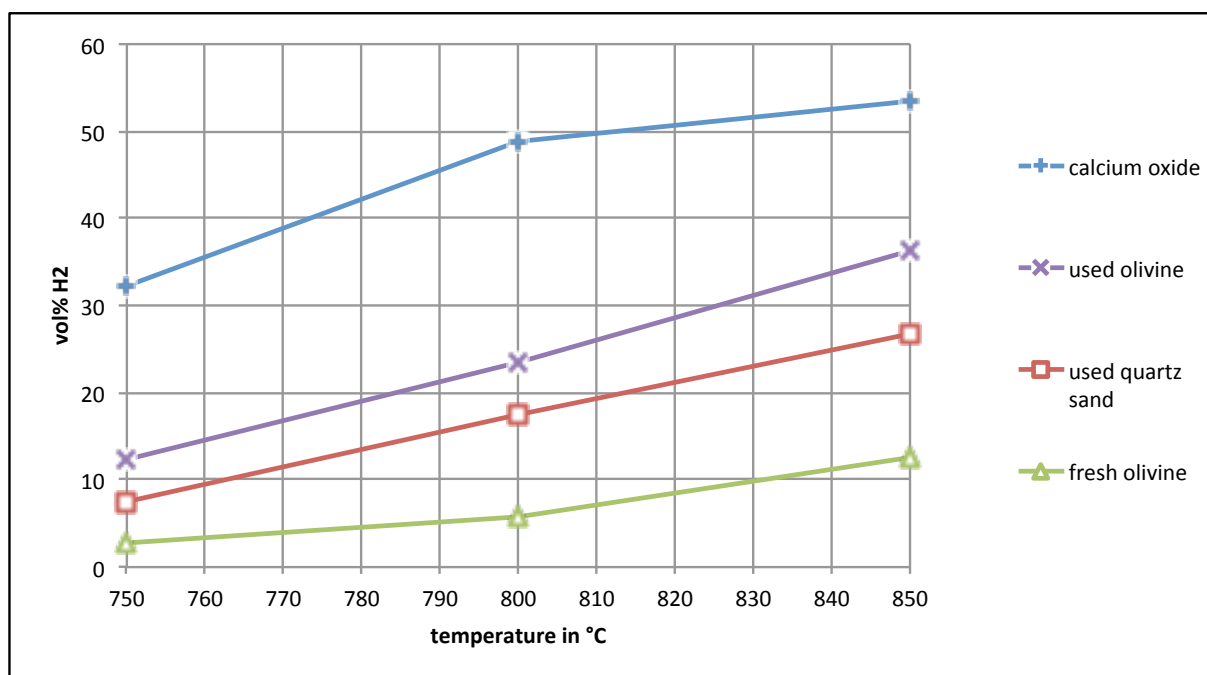


Figure 41: Volumetric proportion of hydrogen in the product gas at a water/toluene ratio of 14/1

4.4 Comparison

Following, results are displayed in diagrams, categorized by bed materials. Figures 42-45 show the volumetric proportion of hydrogen in the product gas. This gives only a qualitative overview, because product gas compositions are influenced by the amount of nitrogen and nitrogen as a carrier gas was not always set to the same flow rate. Consequently, these diagrams show the hydrogen production depending on temperature and allow to compare qualitatively the investigated reactions.

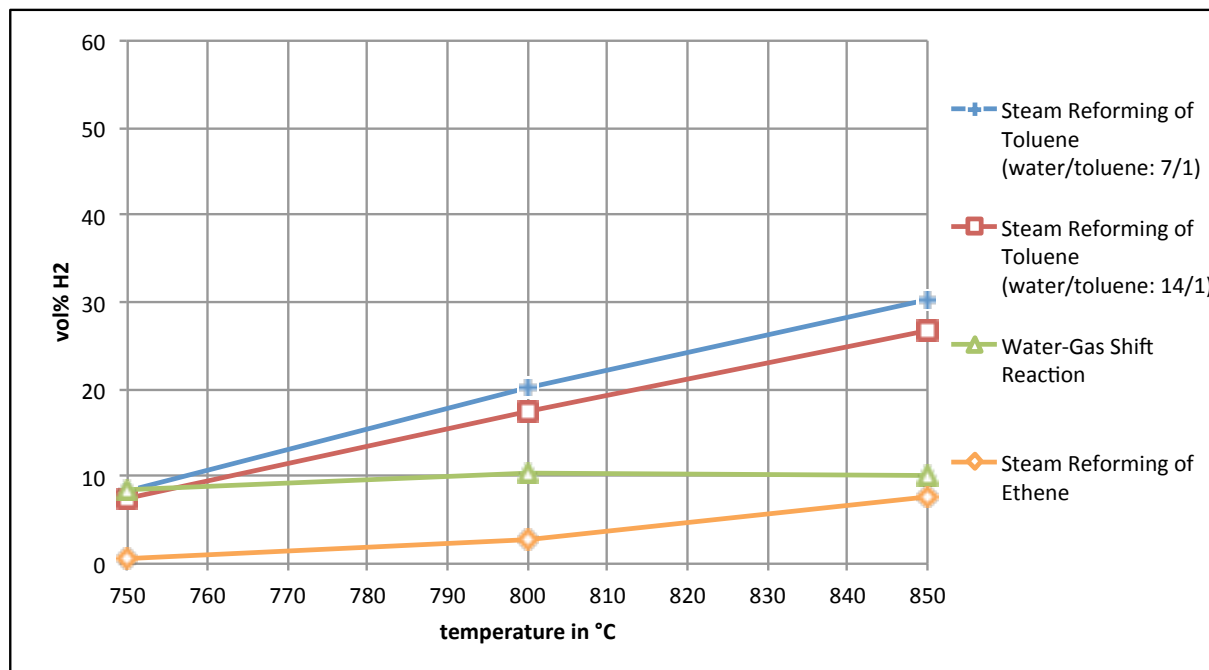


Figure 42: Volumetric proportion of hydrogen with used quartz sand as catalyst

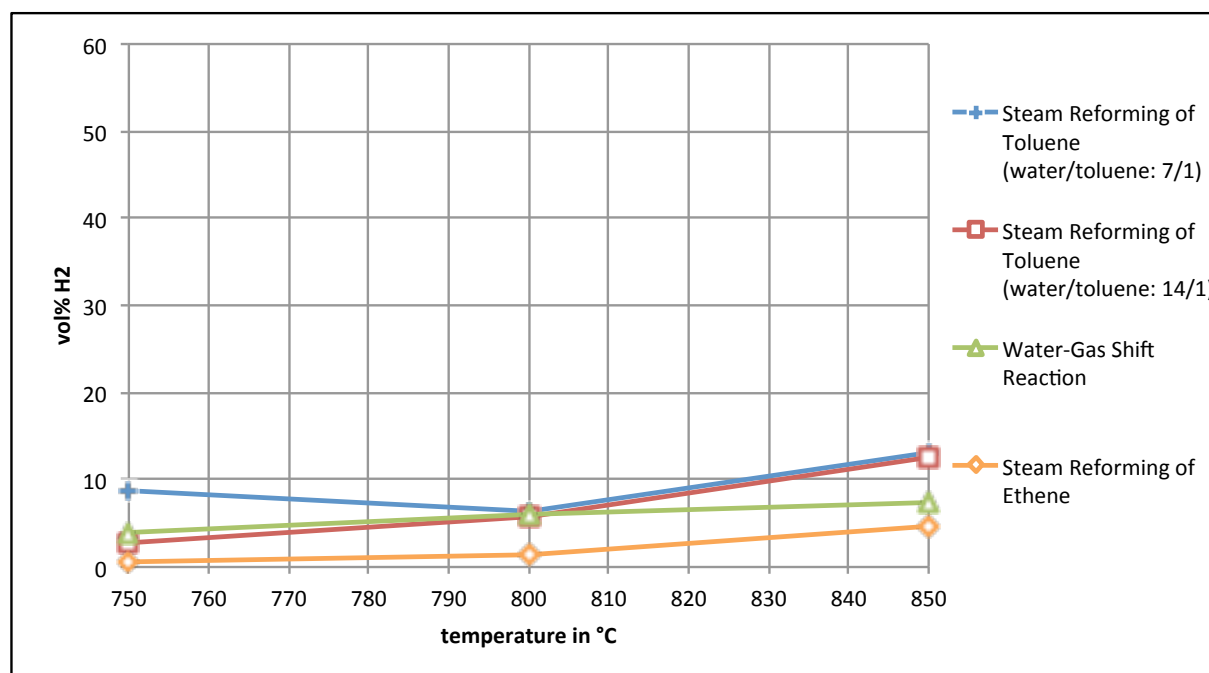


Figure 43: Volumetric proportion of hydrogen with fresh olivine as catalyst

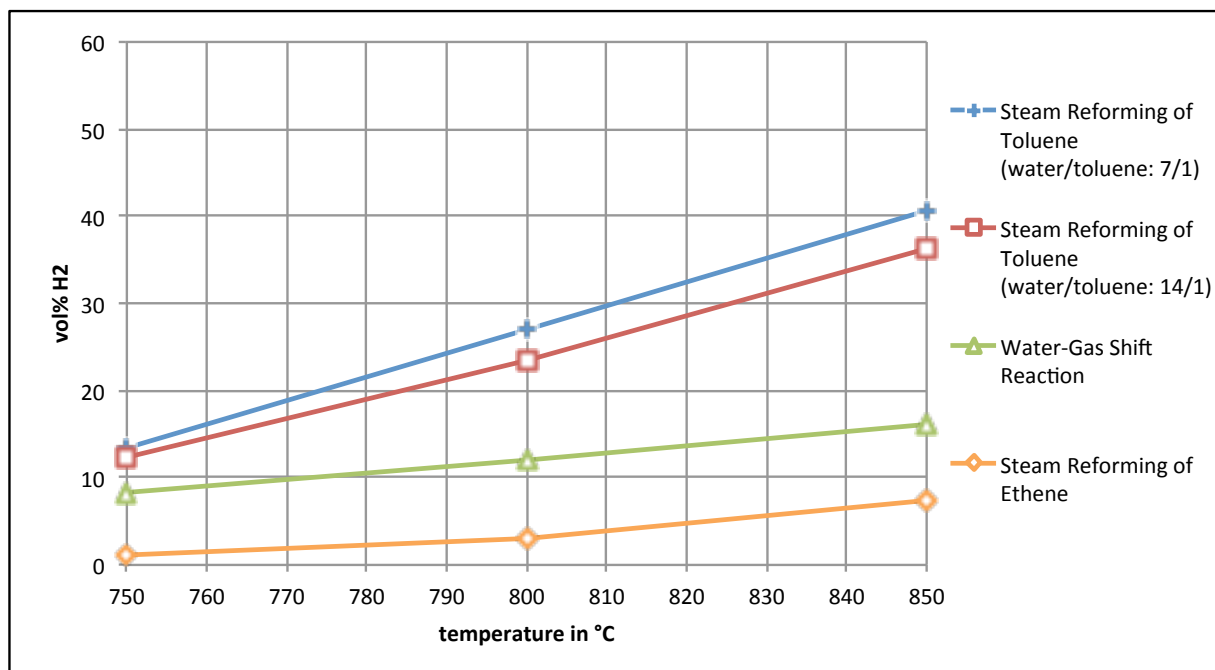


Figure 44: Volumetric proportion of hydrogen with used olivine as catalyst

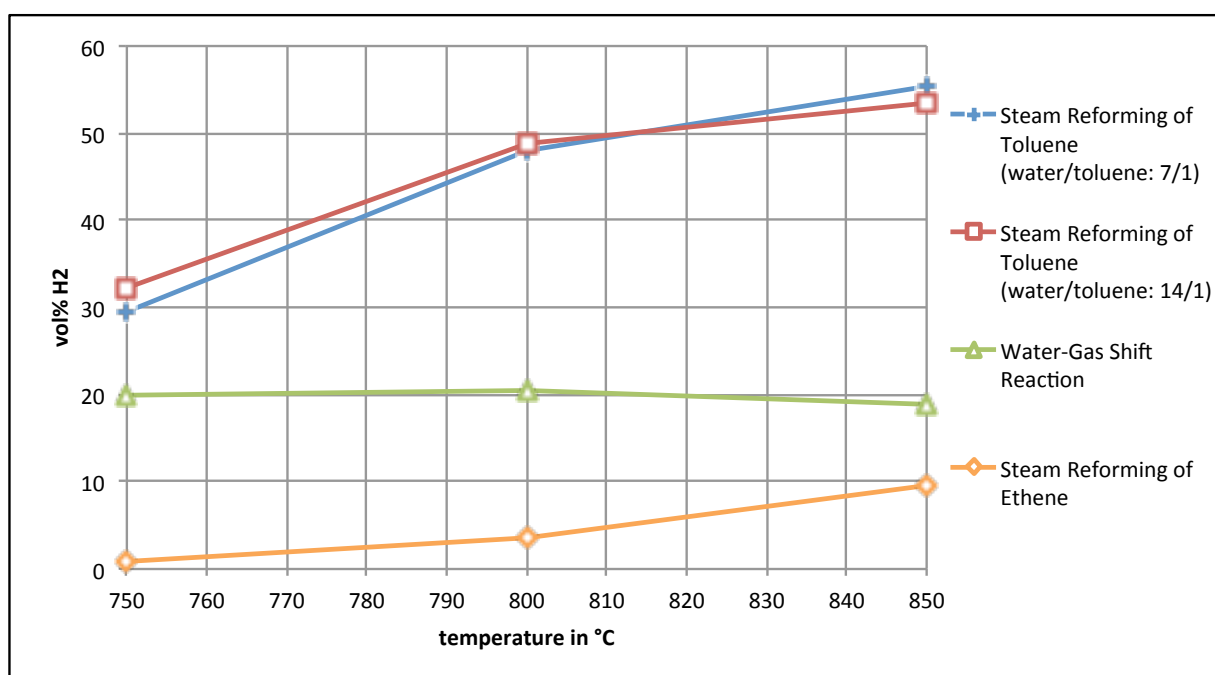


Figure 45: Volumetric proportion of hydrogen with calcium oxide as catalyst

5 Discussion

5.1 Water-Gas Shift Reaction

Results of COCO simulation environment show a higher carbon monoxide conversion at lower temperatures (figure 20). This corresponds to figure 4 (chapter 2). Results from the five component online gas analyzer show a contrary tendency. Figure 26 shows, that – regarding every catalyst but calcium oxide – the conversion rate of carbon monoxide rises with higher temperatures. An explanation could be, that good catalytic effects of the materials start at a certain temperature. The conversion rate of carbon monoxide, using calcium oxide as catalyst, stays constant within some tolerance.

Calcium oxide seems to lead to higher carbon monoxide conversion rates than the equilibrium conversion rate at this temperature. This phenomena could result from the fact, that the five component online gas analyzer is calibrated for low concentrated gas outputs. Therefore, higher volume proportions of carbon monoxide might be measured with an linear error. It can be supposed, that the carbon monoxide conversion rate curve is equal to the calculated equilibrium curve in figure 26.

Another explanation could be the temperature measurement. Temperature is measured at the top of the material filled in the reactor. This material bed is about 7cm tall. It is possible, that the temperature is not steady over the length of the bed. A lower temperature at the bottom of the bed is supposable. Therefore, the temperature of the equilibrium line can not be compared directly with the test results.

Figure 24 shows the hydrogen production rate. In this diagram the hydrogen production rate with calcium oxide as catalyst is almost identical with the equilibrium curve. This better compliance, compared to the carbon monoxide conversion rate (figure 26) might result on different measuring methods of the five component online gas analyzer.

Results show also, that used quartz sand is suitable as a catalyst. Its reactivity for the water-gas shift reaction is in a range between used olivine and fresh olivine. Almost no reactivity show fresh and used CarboHSP and fresh quartz sand. As the composition of fresh and used CarboHSP is not known, no further statement on their low reactivity can

be made. Fresh quartz sand doesn't show catalytic activities. This was expected, because fresh quartz sand doesn't have a calcium-rich layer, which seems to lead to good catalytic properties.

5.2 Steam Reforming of Ethene

Results of COCO simulation environment show a steady conversion rate at temperature ranges, where experiments take place. In figure 27 carbon monoxide production and twice as much hydrogen production occur at temperatures above 700°C. No carbon dioxide should be produced at that temperatures. It can be assumed, that COCO simulation environment doesn't categorize the water-gas shift reaction as an important reaction at high temperatures, because it is an exothermic reaction and should proceed better at lower temperatures. However, water-gas shift reaction tests showed, that the reaction also occurs at high temperatures and emerges at the same time with steam reforming of ethene. Therefore, carbon monoxide is converted and carbon dioxide produced.

Figure 31 shows that hydrogen production depends on temperature. This doesn't conform with results from COCO simulation environment. Probably good catalytic effects of the tested materials start at a certain temperature.

Results show, that reactivity properties of used quartz sand for steam reforming of ethene has almost the same reactivity properties of used olivine. Therefore, used quartz sand would be suitable as catalyst. Almost no reactivity show fresh and used CarboHSP and fresh quartz sand. This fact was also observed at the water-gas shift reaction. As the composition of fresh and used CarboHSP is not known, no further statement on their low reactivity can be made. Fresh quartz sand, which has no calcium-rich layer, doesn't work as a catalyst. Calcium oxide has the best reactivity properties. Nowadays, it is not suitable as bed material for a DFB gasifier because of its bad abrasion properties.

5.3 Steam Reforming of Toluene

These tests were conducted in two modes. First mode is a water/toluene ratio of 7/1 and second mode is a water/toluene ratio of 14/1. In general, a slightly better carbon monoxide, carbon dioxide and hydrogen production is observed at a water/toluene ratio of 7/1. The high water content at a water/toluene ratio of 14/1 might lead to cooling of the reactor and a minimisation of reactivity.

Similar to steam reforming of ethene, results of COCO simulation environment show at a water/toluene ratio of 7/1 steady conversion rates at temperatures above 700°C (figure 32). At a water/toluene ratio of 14/1, conversion rates still change linearly (figure 33). In both cases, the maximally produced gas is hydrogen followed by carbon monoxide. In contrast to a water/toluene ratio of 7/1, water and carbon monoxide occur at a water/toluene ratio of 14/1.

Figure 40 and figure 41 show a better hydrogen production at higher temperatures. According to results of COCO simulation environment (figure 32 and figure 33), the hydrogen production should be steady or falling by increased temperature. Similar to the water-gas shift reaction and steam reforming of ethene, it can be assumed, that good catalytic effects of the materials start at a certain temperature.

Comparing figures 34-39, it is evident, that in all cases a higher amount of carbon dioxide than carbon monoxide was measured. Analogical to steam reforming of ethene, it can be assumed, that COCO simulation environment doesn't categorize the exothermic water-gas shift reaction as an important reaction at high temperatures. However, water-gas shift reaction tests showed, that the reaction also occurs at high temperatures and emerges at the same time with steam reforming of ethene. Therefore, carbon monoxide is converted and carbon dioxide produced.

Results show, that reactivity properties of used quartz sand for steam reforming of toluene has reactivity properties which are in between reactivity properties of used olivine and fresh olivine.

The volume proportions of hydrogen and carbon dioxide are generally high. This results of the little carrier gas stream and produced gases are not highly diluted.

Overall, used quartz sand would be suitable as catalyst. Calcium oxide has the best reactivity properties. Since toluene tests require disproportional more time than water-gas shift or ethene tests, fresh and used CarboHSP and fresh quartz sand were not investigated. It can be expected, that these bed materials show no or a weak reactivity, according to water-gas shift reaction and steam reforming of ethene tests.

5.4 Comparison of Reactions and Bed Material

All three reactions have in common, that at higher temperatures, a higher conversion rate and hydrogen production occurs. If a temperature area favors one of the three examined reactions, it can be assumed, that the other two reactions are favored as well (see figures 42-45).

In every experiment, calcium oxide shows the best catalytic properties. The catalytic activity of used quartz sand is in a range between the activity of used olivine and fresh olivine. Used olivine shows better catalytic properties than fresh olivine.

Results in the appendix show, that the catalytic activities of used quartz sand are strongly alternating in different experiments. Quartz sand was taken from different batches and the operation time of quartz sand was not evident. For further experiments it can be expected, that the catalytic activity of used quartz sand will place in between the catalytic activity of used olivine and fresh olivine.

Very low catalytic activities in all experiments show fresh and used CarboHSP and fresh quartz sand. It was expected, that fresh quartz sand without treatment can not be used as catalyst. By building a calcium-rich layer on quartz sand, the catalytic activities can be changed.

To use quartz sand as bed material in a DFB gasifier, it could be added gradually, by constantly taking out the old bed material. This can be done over a duration of some hours or days to provide enough time for building up a calcium-rich layer on quartz sand particles.

5.5 Error Analysis

5.5.1 Systematic Errors

Temperature Temperature was measured by a thermocouple in the reactor and on the outside wall of the reactor. Measured temperatures usually showed a difference of 30°C to 70°C. For temperature control and data analysis, the inside reactor temperature was taken as reference temperature. The temperature was measured with a precision of 1°C.

Temperature inside the reactor is measured at the top of the material filled in the reactor. This material bed is about 7cm tall. It is possible, that the temperature is not steady over the length of the bed. Knowing from experience, a lower temperature at the bottom of the bed is supposable.

Gas Measurement Gas composition was measured in volume percent. The five component online gas analyzer was calibrated for low concentrated gas streams. Therefore, non-linear errors can occur at higher gas proportions above 20%. An exact limitation of this error can not be given, but it is expected to stay in a certain range of approximately 5%. However, a qualitative comparison among the results is not affected by that error.

5.5.2 Operating and Evaluation Errors

Gas Stream Control Gas streams were controlled by mass flow controllers (MFCs). For experiments, MFCs designed for a maximum of 50Nl/h were used. The minimum flow was limited to 1Nl/h. For water-gas shift and steam reforming of ethene experiments, gas streams from 11Nl/h to 18Nl/h were applied. Since this values are in the operation range of the MFCs, no significant deviations are expected. Steam reforming of toluene required carrier gas streams of 1Nl/h and 1,5Nl/h. This values are close on the border of the operation range. It is possible, that actual gas streams don't accord entirely to the given volume flow rate. However, it is expected, that the deviation of the flow rates of the carrier gas is kept in a small range. Even tough, all toluene experiments were operated at same settings and therefore same deviation errors are expected. A comparison is possible.

Temperature Measurement and Control As a reference temperature, the thermocouple which is installed inside the reactor was taken. A visual check and cleaning after every experiment was done to verify that no sediments settle on the thermocouple. Sediments causes wrong temperature values. Experience has shown, that for all experiments, an error up to -30°C can be assumed.

Since steam reforming of ethene and steam reforming of toluene are endothermic reactions, heat was required. This heat requirement sometimes led to a temperature drop up to -50°C , because heat could not be supplied in fast impulse. This incident required some time (10s to 30s) to reset the operating temperature.

Selection of Values for Operation Point Product gas compositions were measured permanently. The equilibrium in an operation point was defined, by a constant gas composition for a duration more than 10min. This composition was taken for further evaluation of results. An operation error could be, not to wait for equilibrium and taking wrong values for evaluation.

5.5.3 Simplifications

To calculate the carbon monoxide conversion of the water gas shift reaction, it was assumed, that the input of nitrogen equals the output in the product gas. This doesn't apply if leakage occurs, but no significant leakage was found. Furthermore, it was assumed, that nitrogen is the only additional gas beside the measured components. This made quantitative calculations of the product gas proportion possible.

5.5.4 Relevant Errors

Relevant errors are temperature errors and gas stream errors at steam reforming of toluene.

Temperatures mentioned for results could be, according to operation and systematic errors, affected by an inaccuracy up to $\pm 50^{\circ}\text{C}$.

Changes of flow rates of carrier gas at steam reforming of toluene could affect a significant inaccuracy, since the actual flow rates are very small and the product gas proportion comparatively high. Therefore, flow rates were set precisely.

6 Conclusion and Outlook

Biomass gasification is a promising technology for decentralized production of heat, power and synthetic products, such as hydrogen, fuels or chemicals. Olivine is currently used as bed material. It was chosen because of its good catalytic properties, its possibility to act as a heat carrier and its abrasive strength. Olivine also has some disadvantages, which are its higher costs compared to simple bed materials like quartz sand and the matter of fact, that olivine contaminated ash has to be treated as hazardous waste due to chromium and nickel.

In this work, alternative bed materials by considering their catalytic activities, were investigated. Three reactions were carried out with different materials as catalyst. The examined materials were: fresh and used olivine, fresh and used quartz sand, fresh and used CarboHSP and calcium oxide. Used materials were already in use in a fluidized bed combustion or gasification plant and have a calcium-rich surface layer.

Used quartz sand seems to be a promising alternative to olivine. Its catalytic properties were in a range around used olivine and fresh olivine. Its catalytic activity strongly depended on the operation time it was used in the plant. A longer operation time favors a better formation of calcium-rich layers on quartz sand particles. Fresh quartz sand didn't show any catalytic activities, because it possesses no calcium-rich layer.

To use quartz sand as bed material in a DFB gasifier, it could either be prepared by using it as bed material in a combustion fluidized bed reactor or it could be added gradually to the DFB gasifier, by constantly taking out the old bed material. This can be done over a duration of some hours or days to provide enough time for building up a calcium-rich layer on quartz sand particles.

It seems obvious, that coating of the bed material is a relevant factor to improve overall catalytic properties. By comparing used quartz sand and used olivine, good catalytic activities of both materials are noticeable. Nevertheless, exactly the same catalytic activities, relying only on the fact that bed materials are coated, could not be proven by these experiments.

Fresh and used CarboHSP showed only very weak catalytic activities. Calcium oxide had the best catalytic properties. It was taken as a reference. So far, calcium oxide is not suitable as bed material due to its little abrasion resistance.

Water-gas shift reaction, steam reforming of ethene and steam reforming of toluene were the performed reactions. A correlation between the reactions was found. In general, all reactions show a significant better conversion rate at higher temperatures such as 850°C. Lower conversion rates can be observed at lower temperatures at 800°C and 750°C. In addition, the catalytic properties of investigated bed materials stayed the same, no matter which reaction was carried out.

Subsequently to this work, detailed investigations of layers on quartz sand could be carried out. Detailed research, why different samples of used quartz sand show different results, could be made. In addition, steam reforming reactions with heavier hydrocarbons than toluene could be tested and a correlation to experiments from this work could be made.

The next step would be to try quartz sand with a calcium-rich layer as bed material in a small scale DFB gasifier. If tests show good results, upscaling could be done.

References

- [1] Prabir Basu. *Biomass Gasification, Pyrolysis and Torrefaction*. Elsevier Inc., 2013.
- [2] Baofeng Zhao et al. Steam reforming of toluene as model compound of biomass pyrolysis tar for hydrogen. *Biomass and Bioenergy*, 34:140–144, 2009.
- [3] Friedrich Kirnbauer et al. Investigations on bed material changes in a dual fluidized bed steam gasification plant in Güssing, Austria. *Energy and Fuels*, 25:3793–3798, 2011.
- [4] Friedrich Kirnbauer et al. The positive effects of bed material coating on tar reduction in a dual fluidized bed gasifier. *Fuel*, 95:553–562, 2012.
- [5] Friedrich Kirnbauer et al. The mechanism of bed material coating in dual fluidized bed biomass steam gasification plants and its impact on plant optimization. *Powder Technology*, 245:94–104, 2013.
- [6] Hanbing He et al. Time dependence of bed particle layer formation in fluidized quartz bed combustion of wood-derived fuels. *Energy and Fuels*, 28:3841–3848, 2014.
- [7] Hermann Hofbauer et al. Six years experience with the FICFB-gasification process. *12th European Biomass Conference, Amsterdam*, 2002.
- [8] I. Zamboni et al. Simultaneous catalytic H_2 production and CO_2 capture in steam reforming of toluene as tar model compound from biomass gasification. *Applied Catalysis B: Environmental*, 145:63–72, 2013.
- [9] Jun Tao et al. Catalytic steam reforming of toluene as a model compound of biomass gasification tar using $NiCeO_2/SBA - 15$ catalysts. *Energies*, 6:3284–3296, 2013.
- [10] L. Fryda et al. Exergetic analysis of solid oxide fuel cell and biomass gasification integration with heat pipes. *Energy*, 33:292–299, 2008.

-
- [11] M. Zevenhoven-Onderwater et al. The ash chemistry in fluidised bed gasification of biomass fuels. part I: prediction the chemistry of melting ashes and ash-bed material interaction. *Fuel*, 80:1489–1502, 2001.
- [12] M. Zevenhoven-Onderwater et al. The ash chemistry in fluidised bed gasification of biomass fuels. part II: Ash behaviour prediction versus bench scale agglomeration test. *Fuel*, 80:1503–1512, 2001.
- [13] Martin Kaltschmitt et al. *Energie aus Biomasse*. Springer, 2009.
- [14] S. Karellas et al. An innovative biomass gasification process and its coupling with microturbine and fuel cell systems. *Energy*, 33:284–291, 2008.
- [15] S. Papagna et al. Steam-gasification of biomass in a fluidised-bed of olivine particles. *Biomass and Bioenergy*, 19:187–197, 2000.
- [16] Stefan Kern et al. Reactivity tests of the water-gas shift reaction on fresh and used fluidized bed materials from industrial DFB biomass gasifiers. *Biomass and Bioenergy*, 55:227–233, 2013.
- [17] Stefan Koppatz et al. Comparison of the performance behaviour of silica sand and olivine in a dual fluidised bed reactor system for steam gasification of biomass at pilot plant scale. *Chemical Engineering Journal*, 175:468–483, 2011.
- [18] Yasushi Sekine et al. Steam reforming of toluene over perovskite-supported Ni catalysts. *Applied Catalysis A: General*, 451:160–167, 2013.
- [19] Stefan Koppatz. *Outlining active bed materials for dual fluidised bed biomass gasification*. PhD thesis, Vienna University of Technology, 2012.

Appendix A

Results of Water-Gas Shift Reaction Tests

Catalyst: fresh quartz sand, date of experiment: 15.1.2015

set_T °C	TC_T1 °C	CO vol%	CO2 vol%	CH4 vol%	H2 vol%	O2 vol%	set_CO NI/h	set_N2 NI/h	set_H2O g/h	actual_CO NI/h	actual_N2 NI/h	act_H2O g/h	T_steam °C
750	750,2	49,48	0,33	0,05	0,38	-0,02	15	15	12,05	14,98	15,11	12,04	135,0
800	796,7	49,13	0,38	0,05	0,46	0,00	15	15	12,05	14,98	15,11	12,05	135,0
850	848,5	46,01	0,60	0,05	0,67	0,01	15	15	12,05	14,98	15,11	12,05	135,0

notes: used for diagrams in chapter 4

Catalyst: used quartz sand, date of experiment: 20.1.2015

set_T °C	TC_T1 °C	CO vol%	CO2 vol%	CH4 vol%	H2 vol%	O2 vol%	set_CO NI/h	set_N2 NI/h	set_H2O g/h	actual_CO NI/h	actual_N2 NI/h	act_H2O g/h	T_steam °C
750	748,9	45,27	2,90	0,05	3,02	-0,01	15	15	12,05	14,98	15,10	12,05	135,0
800	796,1	41,56	5,08	0,05	5,24	-0,02	15	15	12,05	14,98	15,10	12,04	135,0
850	852,1	38,01	7,13	0,05	7,27	-0,02	15	15	12,05	14,98	15,10	12,04	135,0

notes: -

Catalyst: used quartz sand, date of experiment: 24.10.2014

set_T °C	TC_T1 °C	CO vol%	CO2 vol%	CH4 vol%	H2 vol%	O2 vol%	set_CO NI/h	set_N2 NI/h	set_H2O g/h	actual_CO NI/h	actual_N2 NI/h	act_H2O g/h	T_steam °C
750	751,3	35,78	8,58	0,05	8,49	-0,09	15	15	12,05	14,91	15,11	12,05	135,0
800	802,8	32,93	10,45	0,05	10,29	-0,09	15	15	12,05	14,97	15,11	12,05	135,0
850	847,9	33,00	10,42	0,05	10,23	-0,09	15	15	12,05	14,97	15,11	12,05	135,0

notes: used for diagrams in chapter 4

Catalyst: used quartz sand, date of experiment: 15.12.2014

set_T °C	TC_T1 °C	CO vol%	CO2 vol%	CH4 vol%	H2 vol%	O2 vol%	set_CO NI/h	set_N2 NI/h	set_H2O g/h	actual_CO NI/h	actual_N2 NI/h	act_H2O g/h	T_steam °C
750	766,7	42,75	4,47	0,05	4,58	0,07	15	15	12,05	14,98	15,12	12,05	135,0
800	814,6	38,01	7,42	0,05	7,43	0,07	15	15	12,05	14,98	15,12	12,05	135,0
850	863,5	32,39	10,98	0,05	10,77	0,07	15	15	12,05	14,98	15,06	12,05	135,0

notes: temperatures measured per operation point are around 10°C too high

Catalyst: used quartz sand, date of experiment: 12.2.2015

set_T °C	TC_T1 °C	CO vol%	CO2 vol%	CH4 vol%	H2 vol%	O2 vol%	set_CO NI/h	set_N2 NI/h	set_H2O g/h	actual_CO NI/h	actual_N2 NI/h	act_H2O g/h	T_steam °C
750	747,6	44,12	3,36	0,05	3,50	-0,02	15	15	12,05	14,98	15,08	12,04	135,0
800	798,9	40,02	5,94	0,05	6,00	-0,05	15	15	12,05	14,98	15,08	12,04	135,0
850	850,0	35,61	8,68	0,05	8,62	-0,04	15	15	12,05	14,98	15,08	12,05	135,0

notes: -

Catalyst: used quartz sand, date of experiment: 13.2.2015

set_T °C	TC_T1 °C	CO vol%	CO2 vol%	CH4 vol%	H2 vol%	O2 vol%	set_CO NI/h	set_N2 NI/h	set_H2O g/h	actual_CO NI/h	actual_N2 NI/h	act_H2O g/h	T_steam °C
750	754,1	44,90	3,10	0,05	3,20	-0,08	15	15	12,05	14,98	15,10	12,04	135,0
800	798,5	41,89	4,87	0,05	4,97	-0,09	15	15	12,05	14,98	15,10	12,04	135,0
850	852,7	38,36	6,98	0,05	7,01	-0,09	15	15	12,05	14,98	15,10	12,04	135,0

notes: -

Catalyst: fresh olivine, date of experiment: 17.10.2014

set_T °C	TC_T1 °C	CO vol%	CO2 vol%	CH4 vol%	H2 vol%	O2 vol%	set_CO NI/h	set_N2 NI/h	set_H2O g/h	actual_CO NI/h	actual_N2 NI/h	act_H2O g/h	T_steam °C
750	773,6	43,22	4,17	0,09	3,95	-0,04	15	15	12,05	14,95	15,10	12,04	135,0
800	818,6	40,04	6,00	0,09	6,02	-0,05	15	15	12,05	14,95	15,10	12,04	135,0
850	867,9	37,75	7,42	0,05	7,42	-0,05	15	15	12,05	14,95	15,10	12,04	135,0

notes: used for diagrams in chapter 4, temperatures measured per operation point are around 10°C too high

Catalyst: used olivine, date of experiment: 14.10.2014

set_T °C	TC_T1 °C	CO vol%	CO2 vol%	CH4 vol%	H2 vol%	O2 vol%	set_CO NI/h	set_N2 NI/h	set_H2O g/h	actual_CO NI/h	actual_N2 NI/h	act_H2O g/h	T_steam °C
750	771,6	30,25	11,86	0,09	11,76	-0,06	15	15	12,05	14,96	15,11	12,04	135,0
800	821,0	24,75	15,52	0,09	15,32	-0,07	15	15	12,05	14,96	15,11	12,04	135,0
850	871,0	22,00	17,32	0,09	17,05	-0,07	15	15	12,05	14,96	15,11	12,04	135,0

notes: temperatures measured per operation point are around 20°C too high

Catalyst: used olivine, date of experiment: 5.11.2014

set_T °C	TC_T1 °C	CO vol%	CO2 vol%	CH4 vol%	H2 vol%	O2 vol%	set_CO NI/h	set_N2 NI/h	set_H2O g/h	actual_CO NI/h	actual_N2 NI/h	act_H2O g/h	T_steam °C
750	751,1	37,01	8,40	0,09	8,31	-0,06	15	15	12,05	14,97	15,11	13,01	140,0
800	800,2	30,70	12,28	0,09	12,09	-0,08	15	15	12,05	14,97	15,11	12,83	140,0
850	850,8	23,98	16,47	0,09	16,16	-0,09	15	15	12,05	14,97	15,11	12,91	140,0

notes: used for diagrams in chapter 4, flow rate for water unsteady

Catalyst: fresh CarboHSP, date of experiment: 3.11.2014

set_T °C	TC_T1 °C	CO vol%	CO2 vol%	CH4 vol%	H2 vol%	O2 vol%	set_CO NI/h	set_N2 NI/h	set_H2O g/h	actual_CO NI/h	actual_N2 NI/h	act_H2O g/h	T_steam °C
750	749,1	49,95	0,54	0,09	0,27	-0,07	15	15	12,05	14,97	15,11	12,05	140,0
800	802,5	49,87	0,51	0,09	0,30	-0,07	15	15	12,05	14,97	15,11	12,05	140,0
850	852,8	49,71	0,51	0,09	0,32	-0,07	15	15	12,05	14,97	15,11	12,05	140,0

notes: -

Catalyst: fresh CarboHSP, date of experiment: 9.1.2015

set_T °C	TC_T1 °C	CO vol%	CO2 vol%	CH4 vol%	H2 vol%	O2 vol%	set_CO NI/h	set_N2 NI/h	set_H2O g/h	actual_CO NI/h	actual_N2 NI/h	act_H2O g/h	T_steam °C
750	748,2	48,83	0,52	0,05	0,63	0,07	15	15	12,05	14,98	15,09	12,04	135,0
800	797,7	49,11	0,32	0,05	0,48	0,08	15	15	12,05	14,98	15,09	12,04	135,0
850	849,0	49,29	0,28	0,05	0,42	0,06	15	15	12,05	14,98	15,09	12,04	135,0

notes: used for diagrams in chapter 4

Catalyst: fresh CarboHSP, date of experiment: 13.1.2015

set_T °C	TC_T1 °C	CO vol%	CO2 vol%	CH4 vol%	H2 vol%	O2 vol%	set_CO NI/h	set_N2 NI/h	set_H2O g/h	actual_CO NI/h	actual_N2 NI/h	act_H2O g/h	T_steam °C
750°C	741,5	49,73	0,26	0,05	0,30	0,01	15	15	12,05	14,98	15,11	12,04	135,0
800°C	795,1	49,36	0,35	0,05	0,43	0,01	15	15	12,05	14,98	15,11	12,04	135,0
850°C	846,6	48,77	0,54	0,01	0,66	0,02	15	15	12,05	14,98	15,11	12,04	135,0

notes: -

Catalyst: used CarboHSP, date of experiment: 4.11.2014

set_T °C	TC_T1 °C	CO vol%	CO2 vol%	CH4 vol%	H2 vol%	O2 vol%	set_CO NI/h	set_N2 NI/h	set_H2O g/h	actual_CO NI/h	actual_N2 NI/h	act_H2O g/h	T_steam °C
750	746,7	49,65	0,56	0,09	0,32	-0,06	15	15	12,05	14,97	15,11	12,05	140,0
800	799,3	49,39	0,63	0,09	0,43	-0,07	15	15	12,05	14,97	15,11	12,05	140,0
850	846,5	49,19	0,67	0,09	0,50	-0,07	15	15	12,05	14,97	15,11	12,04	140,0

notes: used for diagrams in chapter 4

Catalyst: calcium oxide, date of experiment: 23.10.2014

set_T °C	TC_T1 °C	CO vol%	CO2 vol%	CH4 vol%	H2 vol%	O2 vol%	set_CO NI/h	set_N2 NI/h	set_H2O g/h	actual_CO NI/h	actual_N2 NI/h	act_H2O g/h	T_steam °C
750	746,7	18,10	19,38	0,05	19,84	-0,05	15	15	12,05	14,96	15,10	12,04	135,0
800	800,1	15,94	21,90	0,05	20,58	-0,05	15	15	12,05	14,96	15,10	12,04	135,0
850	851,2	17,05	23,18	0,08	18,89	-0,07	15	15	12,05	14,96	15,10	12,04	135,0

notes: used for diagrams in chapter 4

Appendix B

Results of Steam Reforming of Ethene Tests

Catalyst: fresh quartz sand, date of experiment: 15.1.2015

set_T °C	TC_T1 °C	CO vol%	CO2 vol%	CH4 vol%	H2 vol%	O2 vol%	set_CO NI/h	set_N2 NI/h	set_H2O g/h	actual_CO NI/h	actual_N2 NI/h	act_H2O g/h	T_steam °C	
750	749,0	0,55	0,09	1,74	0,36	-0,03	11	11	11	18	10,95	11,11	18,00	135,0
800	802,1	0,47	0,08	1,76	0,36	-0,05	11	11	11	18	10,95	11,11	18,00	135,0
850	844,1	0,67	0,11	1,80	1,18	-0,05	11	11	11	18	10,95	11,11	18,00	135,0

notes: used for diagrams in chapter 4

Catalyst: used quartz sand , date of experiment: 24.10.2014

set_T °C	TC_T1 °C	CO vol%	CO2 vol%	CH4 vol%	H2 vol%	O2 vol%	set_CO NI/h	set_N2 NI/h	set_H2O g/h	actual_CO NI/h	actual_N2 NI/h	act_H2O g/h	T_steam °C	
750	744,6	0,12	0,59	2,05	0,55	-0,15	11	11	11	18	10,95	11,11	18,00	135,0
800	796,4	0,23	1,45	2,49	2,90	-0,14	11	11	11	18	10,95	11,11	18,00	135,0
850	844,8	0,82	3,10	3,59	7,77	-0,13	11	11	11	18	10,95	11,11	18,00	135,0

notes: used for diagrams in chapter 4

Catalyst: used quartz sand , date of experiment: 15.12.2014

set_T °C	TC_T1 °C	CO vol%	CO2 vol%	CH4 vol%	H2 vol%	O2 vol%	set_CO NI/h	set_N2 NI/h	set_H2O g/h	actual_CO NI/h	actual_N2 NI/h	act_H2O g/h	T_steam °C	
750	790,1	0,30	0,40	1,90	0,50	0,01	11	11	11	18	10,94	11,11	18,00	135,0
800	837,8	0,49	0,90	2,07	2,52	0,01	11	11	11	18	10,94	11,11	18,00	135,0
850	888,7	0,99	2,38	2,92	7,25	0,02	11	11	11	18	10,95	11,11	18,00	135,0

notes: temperatures measured per operation point are around 40°C too high

Catalyst: used quartz sand , date of experiment: 12.2.2015

set_T °C	TC_T1 °C	CO vol%	CO2 vol%	CH4 vol%	H2 vol%	O2 vol%	set_CO NI/h	set_N2 NI/h	set_H2O g/h	actual_CO NI/h	actual_N2 NI/h	act_H2O g/h	T_steam °C	
750	755,9	0,26	0,12	2,17	-0,18	-0,14	11	11	11	18	10,99	11,08	18,00	135,0
800	797,8	0,30	0,21	2,21	0,18	-0,13	11	11	11	18	10,99	11,09	18,00	135,0
850	849,1	0,48	0,57	2,37	1,57	-0,12	11	11	11	18	10,99	11,08	18,00	135,0

notes: -

Catalyst: used quartz sand , date of experiment: 13.2.2015

set_T °C	TC_T1 °C	CO vol%	CO2 vol%	CH4 vol%	H2 vol%	O2 vol%	set_CO NI/h	set_N2 NI/h	set_H2O g/h	actual_CO NI/h	actual_N2 NI/h	act_H2O g/h	T_steam °C	
750	756,3	0,55	0,12	2,04	-0,04	-0,13	11	11	11	18	10,99	11,10	17,99	135,0
800	802,7	0,36	0,23	2,18	0,43	-0,15	11	11	11	18	10,99	11,10	17,99	135,0
850	851,5	0,54	0,58	2,42	2,02	-0,14	11	11	11	18	10,99	11,10	17,96	135,0

notes: -

Catalyst: fresh olivine , date of experiment: 17.10.2014

set_T °C	TC_T1 °C	CO vol%	CO2 vol%	CH4 vol%	H2 vol%	O2 vol%	set_CO NI/h	set_N2 NI/h	set_H2O g/h	actual_CO NI/h	actual_N2 NI/h	act_H2O g/h	T_steam °C	
750	764,8	0,36	0,31	1,97	0,52	-0,11	11	11	11	18	10,95	11,10	17,99	135,0
800	808,6	0,41	0,54	2,00	1,36	-0,11	11	11	11	18	10,95	11,10	18,00	135,0
850	856,2	1,05	1,27	2,33	4,80	-0,10	11	11	11	18	10,95	11,10	18,00	135,0

notes: used for diagrams in chapter 4

Catalyst: used olivine, date of experiment: 5.11.2014

set_T °C	TC_T1 °C	CO vol%	CO2 vol%	CH4 vol%	H2 vol%	O2 vol%	set_CO NI/h	set_N2 NI/h	set_H2O g/h	actual_CO NI/h	actual_N2 NI/h	act_H2O g/h	T_steam °C
750	746,1	0,08	0,36	2,25	0,00	-0,17	11	11	11	18	10,99	11,11	19,25
800	802,2	0,09	0,73	2,36	0,72	-0,17	11	11	11	18	10,99	11,11	19,05
850	849,0	0,18	1,69	2,58	3,64	-0,16	11	11	11	18	10,99	11,11	19,16

notes: flow rate for water unsteady

Catalyst: used olivine, date of experiment: 9.10.2014

set_T °C	TC_T1 °C	CO vol%	CO2 vol%	CH4 vol%	H2 vol%	O2 vol%	set_CO NI/h	set_N2 NI/h	set_H2O g/h	actual_CO NI/h	actual_N2 NI/h	act_H2O g/h	T_steam °C
790°C	785,7	0,05	0,52	44,90	1,87	1,755876	11	11	11	18,00	10,99	11,10	17,99
840°C	840,0	0,13	0,56	44,28	2,61	1,744136	11	11	11	18,00	10,99	11,10	17,99
890°C	895,8	0,22	0,74	43,67	4,05	1,473312	11	11	11	18,00	10,99	11,11	17,99

notes: temperatures measured per operation point are around 40°C too high

Catalyst: used olivine, date of experiment: 20.10.2014

set_T °C	TC_T1 °C	CO vol%	CO2 vol%	CH4 vol%	H2 vol%	O2 vol%	set_CO NI/h	set_N2 NI/h	set_H2O g/h	actual_CO NI/h	actual_N2 NI/h	act_H2O g/h	T_steam °C
750	748,3	0,15	0,74	2,41	1,03	-0,02	11	11	11	18	10,99	11,10	17,99
800	794,5	0,17	1,51	2,61	3,04	0,01	11	11	11	18	10,99	11,10	18,00
850	832,3	0,62	2,88	3,31	7,47	0,02	11	11	11	18	10,99	11,10	18,00

notes: used for diagrams in chapter 4

Catalyst: fresh CarboHSP, date of experiment: 3.11.2014

set_T °C	TC_T1 °C	CO vol%	CO2 vol%	CH4 vol%	H2 vol%	O2 vol%	set_CO NI/h	set_N2 NI/h	set_H2O g/h	actual_CO NI/h	actual_N2 NI/h	act_H2O g/h	T_steam °C	
750	749,1	0,09	0,16	2,25	-0,88	-0,17	11	11	11	18	10,99	11,11	18,00	140,0
800	799,5	0,13	0,19	2,26	-0,59	-0,16	11	11	11	18	10,99	11,11	18,00	140,0
850	849,3	0,32	0,28	2,44	0,71	-0,16	11	11	11	18	10,99	11,11	17,54	140,0

notes: -

Catalyst: fresh CarboHSP, date of experiment: 9.1.2015

set_T °C	TC_T1 °C	CO vol%	CO2 vol%	CH4 vol%	H2 vol%	O2 vol%	set_CO NI/h	set_N2 NI/h	set_H2O g/h	actual_CO NI/h	actual_N2 NI/h	act_H2O g/h	T_steam °C	
750	750,0	0,42	0,08	2,14	0,04	-0,02	11	11	11	18	10,99	11,08	18,00	135,0
800	798,6	0,54	0,06	2,14	0,33	-0,05	11	11	11	18	10,99	11,08	18,00	135,0
850	845,2	0,61	0,05	2,29	1,16	-0,02	11	11	11	18	10,99	11,08	18,00	135,0

notes: used for diagrams in chapter 4

Catalyst: used CarboHSP, date of experiment: 4.11.2014

set_T °C	TC_T1 °C	CO vol%	CO2 vol%	CH4 vol%	H2 vol%	O2 vol%	set_CO NI/h	set_N2 NI/h	set_H2O g/h	actual_CO NI/h	actual_N2 NI/h	act_H2O g/h	T_steam °C	
750	750,9	0,14	0,15	2,22	0,00	-0,17	11	11	11	18	10,99	11,11	18,00	140,0
800	800,2	0,20	0,15	2,26	0,00	-0,18	11	11	11	18	10,99	11,11	18,00	140,0
850	851,1	0,38	0,19	2,35	0,54	-0,17	11	11	11	18	10,99	11,11	18,00	140,0

notes: used for diagrams in chapter 4

Catalyst: calcium oxide, date of experiment: 23.10.2014

set_T °C	TC_T1 °C	CO vol%	CO2 vol%	CH4 vol%	H2 vol%	O2 vol%	set_CO NI/h	set_N2 NI/h	set_H2O g/h	actual_CO NI/h	actual_N2 NI/h	act_H2O g/h	T_steam °C	
750	745,3	0,09	4,58	2,71	0,84	-0,15	11	11	11	18	10,99	11,10	18,00	135,0
800	800,6	0,20	8,22	3,65	3,60	-0,15	11	11	11	18	10,99	11,10	18,00	135,0
850	847,4	0,73	9,19	5,67	9,50	-0,13	11	11	11	18	10,99	11,10	18,00	135,0

notes: used for diagrams in chapter 4

Appendix C

Results of Steam Reforming of Toluene Tests

(water/toluene ratio: 7/1)

Catalyst: used quartz sand, water/toluene ratio: 7/1, date of experiment: 22.1.2015

set_T °C	TC_T1 °C	CO vol%	CO2 vol%	CH4 vol%	H2 vol%	O2 vol%	setN2,H2O setN2,Tol NI/h	set_H2O g/h	actN2,H2O actN2,Tol NI/h	act_H2O g/h	T_steam °C	act_C7H8 ml/h	H2O_out ml/min	C7H8_out ml/min
750	732,9	1,71	1,25	0,92	8,34	0,80	1,5	1	25,22	1,60	0,98	135,00	21,18	0,15
800	814,5	5,12	4,35	0,50	20,12	0,44	1,5	1	25,22	1,60	0,98	135,00	21,18	0,39
850	855,3	8,31	6,41	0,58	30,25	0,47	1,5	1	25,22	1,60	0,98	135,00	21,18	0,46

notes: used for diagrams in chapter 4

Catalyst: used quartz sand, water/toluene ratio: 7/1, date of experiment: 16.2.2015

set_T °C	TC_T1 °C	CO vol%	CO2 vol%	CH4 vol%	H2 vol%	O2 vol%	setN2,H2O setN2,Tol NI/h	set_H2O g/h	actN2,H2O actN2,Tol NI/h	act_H2O g/h	T_steam °C	act_C7H8 ml/h	H2O_out ml/min	C7H8_out ml/min
750	759,1	1,07	0,67	0,09	3,57	0,81	1,5	1	25,22	1,60	0,97	135,00	21,18	0,06
800	804,9	1,72	1,41	0,20	6,84	0,59	1,5	1	25,22	1,60	0,97	135,00	21,18	0,27
850	847,8	2,81	2,85	0,42	12,59	0,73	1,5	1	25,22	1,60	0,97	135,00	21,18	0,47

notes: -

Catalyst: fresh olivine, water/toluene ratio: 7/1, date of experiment: 18.12.2014

set_T °C	TC_T1 °C	CO vol%	CO2 vol%	CH4 vol%	H2 vol%	O2 vol%	setN2,H2O setN2,Tol NI/h	set_H2O g/h	actN2,H2O actN2,Tol NI/h	act_H2O g/h	T_steam °C	act_C7H8 ml/h	H2O_out ml/min	C7H8_out ml/min
750	741,7	3,00	1,21	0,24	8,67	0,85	1,5	1	25,22	1,60	0,98	134,99	21,18	0,14
800	794,4	2,71	0,76	0,28	6,39	0,63	1,5	1	25,22	1,60	0,98	135,00	21,18	0,13
850	853,0	5,50	1,15	2,61	13,13	0,71	1,5	1	25,22	1,60	0,98	135,00	21,18	0,28

notes: used for diagrams in chapter 4

Catalyst: used olivine, water/toluene ratio: 7/1, date of experiment: 16.12.2014

set_T °C	TC_T1 °C	CO vol%	CO2 vol%	CH4 vol%	H2 vol%	O2 vol%	setN2,N2, Tol NI/h	set_H2O g/h	actN2,N2, Tol NI/h	act_H2O g/h	T_steam °C	act_C7H8 ml/h	H2O_out ml/min	C7H8_out ml/min
750	745,9	0,62	4,43	0,21	13,32	0,67	1,5	1	1,60	0,98	25,22	135,01	21,18	0,27
800	791,2	1,35	9,15	0,38	27,09	0,51	1,5	1	1,60	0,98	25,22	135,00	21,18	0,23
850	845,7	2,28	13,91	0,86	40,67	0,37	1,5	1	1,60	0,98	25,22	135,00	21,18	0,23

notes: used for diagrams in chapter 4

Catalyst: calcium oxide, water/toluene ratio: 7/1, date of experiment: 19.12.2014

set_T °C	TC_T1 °C	CO vol%	CO2 vol%	CH4 vol%	H2 vol%	O2 vol%	setN2,H2O setN2,Tol NI/h	set_H2O g/h	actN2,H2O actN2,Tol NI/h	act_H2O g/h	T_steam °C	act_C7H8 ml/h	H2O_out ml/min	C7H8_out ml/min
750	751,3	1,19	29,38	0,41	29,40	0,43	1,5	1	1,62	0,97	25,22	135,01	21,18	0,13
800	800,4	3,19	24,04	1,20	47,89	0,33	1,5	1	1,62	0,97	25,22	134,99	21,18	0,47
850	851,7	6,53	19,39	1,81	55,33	0,25	1,5	1	1,62	0,97	25,23	135,00	21,18	0,30

notes: used for diagrams in chapter 4

Appendix D

Results of Steam Reforming of Toluene Tests

(water/toluene ratio: 14/1)

Catalyst: used quartz sand, water/toluene ratio: 14/1, date of experiment: 22.1.2015

set_T °C	TC_T1 °C	CO vol%	CO2 vol%	CH4 vol%	H2 vol%	O2 vol%	setN2, H2O setN2, Tol NI/h	set_H2O g/h	actN2, H2O actN2, Tol NI/h	act_H2O g/h	T_steam °C	act_C7H8 ml/h	H2O_out ml/min	C7H8_out ml/min	
750	734,5	1,23	2,00	0,39	7,49	0,77	1,5	1	25,22	1,60	0,98	135,0	10,59	0,38	0,11
800	803,3	4,79	4,20	0,46	17,49	0,60	1,5	1	25,22	1,60	0,98	135,0	10,59	0,25	0,09
850	841,0	7,32	5,75	0,53	26,88	0,34	1,5	1	25,22	1,60	0,98	135,0	10,59	0,43	0,11

notes: used for diagrams in chapter 4

Catalyst: used quartz sand, water/toluene ratio: 14/1, date of experiment: 16.2.2015

set_T °C	TC_T1 °C	CO vol%	CO2 vol%	CH4 vol%	H2 vol%	O2 vol%	setN2, H2O setN2, Tol NI/h	set_H2O g/h	actN2, H2O actN2, Tol NI/h	act_H2O g/h	T_steam °C	act_C7H8 ml/h	H2O_out ml/min	C7H8_out ml/min	
750	776,4	0,88	0,76	0,09	3,30	0,96	1,5	1	25,22	1,60	0,97	135,0	10,59	0,39	0,07
800	801,4	1,80	1,49	0,16	6,73	1,01	1,5	1	25,22	1,60	0,97	135,0	10,59	0,48	0,17
850	849,2	2,65	2,50	0,40	10,96	0,45	1,5	1	25,22	1,60	0,97	135,0	10,59	0,44	0,12

notes: -

Catalyst: fresh olivine, water/toluene ratio: 14/1, date of experiment: 18.12.2014

set_T °C	TC_T1 °C	CO vol%	CO2 vol%	CH4 vol%	H2 vol%	O2 vol%	setN2, H2O setN2, Tol NI/h	set_H2O g/h	actN2, H2O actN2, Tol NI/h	act_H2O g/h	T_steam °C	act_C7H8 ml/h	H2O_out ml/min	C7H8_out ml/min	
750	750,6	1,11	0,44	0,10	2,63	0,65	1,5	1	25,22	1,60	0,98	135,0	10,59	0,18	0,04
800	805,3	2,67	0,65	0,20	5,71	0,85	1,5	1	25,22	1,60	0,98	135,0	10,59	0,20	0,26
850	853,5	5,16	1,14	2,56	12,52	0,75	1,5	1	25,22	1,60	0,98	135,0	10,59	n.a.	n.a.

notes: used for diagrams in chapter 4, toluene and water condensate were not measured at 850°C

Catalyst: used olivine, water/toluene ratio: 14/1, date of experiment: 16.12.2014

set_T °C	TC_T1 °C	CO vol%	CO2 vol%	CH4 vol%	H2 vol%	O2 vol%	setN2,N2 setN2,N2 NI/h	set_H2O g/h	actN2,N2 actN2,N2 NI/h	act_H2O g/h	T_steam °C	act_C7H8 ml/h	H2O_out ml/min	C7H8_out ml/min
750	751,3	0,64	12,33	0,17	12,33	0,60	1,5	25,22	1,60	0,98	25,23	135,0	10,59	0,36
800	802,5	0,96	23,60	0,36	23,60	0,56	1,5	25,22	1,60	0,98	25,23	135,0	10,59	0,25
850	851,0	1,65	36,30	0,67	36,30	0,39	1,5	25,22	1,60	0,98	25,22	135,0	10,59	0,30

notes: used for diagrams in chapter 4

Catalyst: calcium oxide, water/toluene ratio: 14/1, date of experiment: 19.12.2014

set_T °C	TC_T1 °C	CO vol%	CO2 vol%	CH4 vol%	H2 vol%	O2 vol%	setN2,H2O setN2,Tol NI/h	set_H2O g/h	actN2,H2O actN2,Tol NI/h	act_H2O g/h	T_steam °C	act_C7H8 ml/h	H2O_out ml/min	C7H8_out ml/min
750	755,9	1,13	32,22	0,63	32,22	0,49	1,5	25,22	1,62	0,97	25,22	135,0	10,59	0,22
800	811,5	3,21	48,82	0,88	48,82	0,34	1,5	25,22	1,61	0,97	25,22	135,0	10,59	0,35
850	843,4	5,37	53,48	1,27	53,48	0,28	1,5	25,22	1,62	0,97	25,22	135,0	10,59	0,22

notes: used for diagrams in chapter 4